HIF-1α is overexpressed in leukemic cells from TP53-disrupted patients and is a promising therapeutic target in chronic lymphocytic leukemia

haematologica
Journal of The Ferrata Storti Foundation

HIF-1α is overexpressed in leukemic cells from TP53-disrupted patients and is a promising therapeutic target in chronic lymphocytic leukemia

by Valentina Griggio, Candida Vitale, Maria Todaro, Chiara Riganti, Joanna Kopecka, Chiara Salvetti, Riccardo Bomben, Michele Dal Bo, Daniela Magliulo, Davide Rossi, Gabriele Pozzato, Lisa Bonello, Monia Marchetti, Paola Omedè, Ahad Ahmed Kodipad, Luca Laurenti, Giovanni Del Poeta, Francesca Romana Mauro, Rosa Bernardi, Thorsten Zenz, Valter Gattei, Gianluca Gaidano, Robin Foà, Massimo Massaia, Mario Boccadoro, and Marta Coscia

Haematologica 2019 [Epub ahead of print]

Citation: Valentina Griggio, Candida Vitale, Maria Todaro, Chiara Riganti, Joanna Kopecka, Chiara Salvetti, Riccardo Bomben, Michele Dal Bo, Daniela Magliulo, Davide Rossi, Gabriele Pozzato, Lisa Bonello, Monia Marchetti, Paola Omedè, Ahad Ahmed Kodipad, Luca Laurenti, Giovanni Del Poeta, Francesca Romana Mauro, Rosa Bernardi, Thorsten Zenz, Valter Gattei, Gianluca Gaidano, Robin Foà, Massimo Massaia, Mario Boccadoro, and Marta Coscia. HIF-1α is overexpressed in leukemic cells from TP53-disrupted patients and is a promising therapeutic target in chronic lymphocytic leukemia. Haematologica. 2019; 104:xxx doi:10.3324/haematol.2019.217430

Title Page

Article title: HIF-1α is overexpressed in leukemic cells from *TP53*-disrupted patients and is a promising therapeutic target in chronic lymphocytic leukemia

Running head: HIF-1α in *TP53*-disrupted CLL Cells

Authors: Valentina Griggio[1,2], Candida Vitale[1,2], Maria Todaro[1,2], Chiara Riganti[3], Joanna Kopecka[3], Chiara Salvetti[1,2], Riccardo Bomben[4], Michele Dal Bo[4], Daniela Magliulo[5], Davide Rossi[6], Gabriele Pozzato[7], Lisa Bonello[2], Monia Marchetti[8], Paola Omedè[1], Ahad Ahmed Kodipad[9], Luca Laurenti[10], Giovanni Del Poeta[11], Francesca Romana Mauro[12]; Rosa Bernardi[5], Thorsten Zenz[13], Valter Gattei[4], Gianluca Gaidano[9], Robin Foà[12], Massimo Massaia[14], Mario Boccadoro[1,2] and Marta Coscia[1,2]

Affiliations:

[1]Division of Hematology, A.O.U. Città della Salute e della Scienza di Torino, Turin, Italy; [2]Department of Molecular Biotechnology and Health Sciences, University of Torino, Torino, Italy

[3]Department of Oncology, University of Torino, Turin, Italy

[4]Clinical and Experimental Onco-Hematology Unit, CRO Aviano National Cancer Institute, Aviano, Italy

[5]Division of Experimental Oncology, IRCCS San Raffaele Scientific Institute, Milan, Italy; [6]Department of Hematology, Oncology Institute of Southern Switzerland and Institute of Oncology Research, Bellinzona, Switzerland

[7]Department of Internal Medicine and Hematology, Maggiore General Hospital, University of Trieste, Trieste, Italy

[8]Hematology Day Service, Oncology SOC, Hospital Cardinal Massaia, Asti, Italy

[9]Division of Hematology, Department of Translational Medicine, University of Eastern Piedmont, Novara, Italy

[10]Fondazione Policlinico Universitario Agostino Gemelli, Rome, Italy

[11]Division of Hematology, S. Eugenio Hospital and University of Tor Vergata, Rome, Italy

[12]Hematology, Department of Translational and Precision Medicine, Sapienza University, Policlinico Umberto I, Rome, Italy

[13]Department of Medical Oncology and Hematology, University Hospital and University of Zurich, Zurich, Switzerland

[14]Hematology Unit, ASO Santa Croce e Carle, Cuneo, Italy

Corresponding Author: Dr. Marta Coscia, Division of Hematology, Department of Molecular Biotechnology and Health Sciences, University of Torino, Azienda Ospedaliero-Universitaria Città della Salute e della Scienza di Torino, via Genova 3, 10126 Torino, Italy. Phone Number: +390116336728; Fax Number: +390116963737; e-mail address: marta.coscia@unito.it

V.Griggio and C.V. contributed equally to this study.

Word count: 3801

Tables and Figures: 7

Supplemental files: 1

Acknowledgements

The authors would like to thank: Italian Association for Cancer Research (AIRC IG15232 and IG21408) (C.R.), (AIRC IG13119, AIRC IG16985, AIRC IG2174) (M.Massaia), (AIRC IG17622) (V.Gattei), (AIRC 5x1000 project 21198, Metastatic disease: the key unmet need in oncology) (G.G) (AIRC 5x1000 Special Programs MCO-10007 and 21198) (R.F.); Fondazione Neoplasie Sangue (Fo.Ne.Sa), Torino, Italy; University of Torino (local funds ex-60%) (M.C.); Ministero della Salute, Rome, Italy (Progetto Giovani Ricercatori GR-

2011-02347441 [R.Bomben], GR-2009-1475467 [R.Bomben], and GR-2011-02351370 [M.DB.]). Fondazione Cassa di Risparmio di Torino (CRT) (V.Griggio was recipient of a fellowship), Fondazione “Angela Bossolasco” Torino, Italy (V.Griggio was recipient of the “Giorgio Bissolotti e Teresina Bosio” fellowship), the Italian Association for Cancer Research (AIRC, Ref 16343 V.Griggio was recipient of the “Anna Nappa” fellowship and M.T. is currently the recipient of a fellowship from AIRC Ref 19653). Associazione Italiana contro le Leucemie, Linfomi e Mieloma (AIL) (C.V. was recipient of a fellowship).

Abstract

In chronic lymphocytic leukemia, the hypoxia-inducible factor 1 (HIF-1) regulates the response of tumour cells to hypoxia and their protective interactions with the leukemic microenvironment. In this study we demonstrate that chronic lymphocytic leukemia cells from *TP53*-disrupted (*TP53*^{dis}) patients have constitutively higher expression levels of the α-subunit of HIF-1 (HIF-1α) and increased HIF-1 transcriptional activity, compared to the wild type counterpart. In the *TP53*^{dis} subset, HIF-1α upregulation is due to reduced expression of the HIF-1α ubiquitin ligase von Hippel-Lindau protein (pVHL). Hypoxia and stromal cells further enhance HIF-1α accumulation, independently from the *TP53* status. Hypoxia acts through the downmodulation of pVHL and the activation of the PI3K/AKT and RAS/ERK1-2 pathways, whereas stromal cells induce an increased activity of the RAS/ERK1-2, RHOA/RHOA kinase and PI3K/AKT pathways, without affecting pVHL expression. Interestingly, we observed that higher levels of *HIF-1A* mRNA correlate with a lower susceptibility of leukemic cells to spontaneous apoptosis, and associate with the fludarabine resistance that mainly characterizes *TP53*^{dis} tumour cells. The HIF-1α inhibitor BAY87-2243 exerts cytotoxic effects toward leukemic cells, regardless of the *TP53* status, and has anti-tumour activity in Eμ-TCL1 mice. BAY87-2243 also overcomes the constitutive fludarabine resistance of *TP53*^{dis} leukemic cells and elicits a strongly synergistic cytotoxic effect in combination with ibrutinib, thus providing preclinical evidences for its further investigation as a potential new drug in chronic lymphocytic leukemia.

Article summary

1) The aim of this study is two-fold: i) to unravel HIF-1α regulatory pathways in chronic lymphocytic leukemia cells (CLL) from *TP53*-disrupted and wild type patients; ii) to provide preclinical evidences for the anti-tumour activity of the HIF-1α inhibitor BAY87-2243 in CLL.
2) HIF-1α is overexpressed in leukemic cells from *TP53*-disrupted CLL patients, and is further upregulated by hypoxia and stromal cells. The HIF-1α inhibitor BAY87-2243 exerts cytotoxic effects toward leukemic cells, sensitizes *TP53*-disrupted CLL cells to fludarabine and synergizes with ibrutinib.

Introduction

Chronic lymphocytic leukemia (CLL) patients with high-risk genomic features such as disruption of the *TP53* gene (i.e. del(17p) and *TP53* mutations) respond poorly to chemoimmunotherapy and frequently relapse[1–9]. Significant advances have been made in the treatment of CLL following the introduction of Bruton tyrosine kinase (BTK) inhibitors[10]. Ibrutinib, which is currently approved for the front-line treatment of CLL, induces long-lasting responses in the majority of patients, improving outcome with relatively limited toxicities[10]. However, patients with disruption of the *TP53* gene (*TP53*^{dis}) treated with ibrutinib are still characterized by a poorer outcome[11].

Hypoxia inducible factor 1 (HIF-1) is an essential regulator of cell adaptation to hypoxia and is often upregulated in tumours due to intratumoural hypoxia or activation of oncogenic pathways[12,13]. In tumours, HIF-1 fosters different tumour-promoting mechanisms, including metabolic adaptation, neoangiogenesis, cell survival and invasion[14].

HIF-1 is a heterodimer, which consists of a constitutively expressed HIF-1β subunit and an inducible HIF-1α subunit. Besides its traditional regulation via proteasomal degradation, other signalling pathways, such as PI3K/AKT and RAS/ERK1-2, contribute to HIF-1α accumulation, via stability regulation or synthesis induction[12,15].

HIF-1α is constitutively expressed in CLL cells compared to normal B cells due to microRNA-mediated downregulation of the von Hippel-Lindau protein (pVHL)[16], a ubiquitin ligase responsible for HIF-1α degradation[12]. In addition, in CLL cells HIF-1α is upregulated by the interactions with stromal cells (SC) and by exposure to hypoxic microenvironments, thus promoting the survival and propagation of leukemic cells, and their metabolic adaptation to the protective conditions of the tumour niche[17–20]. We have already reported that HIF-1α is involved in drug resistance mechanisms in patients with unmutated (UM) immunoglobulin heavy chain variable region genes (IGHV)[20]. *TP53* gene encodes one of

the most well-studied tumour suppressor protein, which is often mutated in cancer, thus promoting cell survival, proliferation and drug resistance[21]. p53 may also play a pivotal role in the regulation of HIF-1α, since in conditions of prolonged hypoxia/anoxia the protein accumulates and promotes HIF-1α destruction[22]. In solid tumours, loss of *TP53* function associates with constitutive elevated levels of HIF-1α[12,22,23].

In this study, we found that HIF-1α is overexpressed in CLL cells from patients carrying *TP53* aberrations, also elucidating the molecular mechanisms implicated in the constitutive (*TP53*-related) and inducible (hypoxia- and SC-induced) HIF-1α upregulation. In addition, we documented that the HIF-1α inhibitor BAY87-2243 exerts potent anti-tumour functions, overcoming the constitutive fludarabine resistance of *TP53*-disrupted CLL cells and eliciting a strong synergistic cytotoxic effect in combination with ibrutinib.

Methods

Patients' samples

A total of 102 patients with CLL, diagnosed according to the International Workshop on CLL-National Cancer Institute guidelines[24], were included in the study (40 $TP53^{dis}$ and 62 *TP53*-wild type [$TP53^{wt}$] cases) (Table 1 in Supplemental Information). Healthy donors' (HD, n=2) samples were provided by the local blood bank. Patients were untreated or off-therapy for at least 12 months before sampling of peripheral blood (PB) for the experiments. Samples were collected after patients' informed consent, in accordance with the Declaration of Helsinki and approval by the local Institutional Review Board. PB mononuclear cells (PBMC) were isolated and characterized as detailed in Supplemental Information.

Cell lines

The Burkitt's lymphoma cell line, Séraphine, and the mantle cell lymphoma cell line, Granta-519, were kindly provided by T. Zenz. In the study the $TP53^{wt}$ and the

CRISPR/Cas9-mediated *TP53* knockout version (*TP53*^{ko}) of Granta-519 and Séraphine cell lines were used. The M2-10B4 murine SC line (ATCC #CRL-1972) was also used. Cell lines were maintained as reported in Supplemental Information.

Animals

C57BL/6 Eμ-TCL1 mice were maintained in specific pathogen-free animal facilities and treated in accordance with European Union guidelines and Institutional Animal Care and Use Committee (number 716). Splenic cells ($5x10^6$) were injected intraperitoneally into syngeneic C57BL/6 mice, and experiments were performed with 4-6 mice groups. Leukemic mice were treated when tumour cells reached 10% in PB. BAY87-2243 was administered 4 mg/kg in ethanol/solutol/water solution once daily by oral gavage. Mice were sacrificed at the end of treatment.

Cell culture

In selected experiments, CLL cells were cultured in the presence or absence of M2-10B4 SC, and exposed to PD98059 (Sigma Aldrich, Milan), Y27632 (Sigma Aldrich) or LY249002 (Sellekchem, Houston, TX) for 48 hours. CLL cells were exposed for 48 hours to BAY87-2243 (Sellekchem); 2-Fluoroadenine-9-β-D-arabinofuranoside (F-ara-A, Sigma Aldrich); ibrutinib (Sellekchem) used alone or in combination, at the indicated concentrations. Culture conditions were normoxia or mild hypoxia (1% O_2), 5% CO_2 at 37°C.

Western blot (WB)

Full details can be found in Supplemental Information together with the list of antibodies used for WB analyses.

Quantitative real-time PCR

Full details can be found in Supplemental Information together with the list of primers sequences.

Gene set enrichment analysis

"Gene Set Enrichment Analysis" (GSEA, http://www.broad.mit.edu/gsea/index.jsp) was performed as previously described[25,26]. Gene sets were assessed as significantly enriched in one of the phenotypes if the nominal p value and the FDR-q value were less than 0.05.

RHOA and RAS, ERK1-2, AKT and RHOA kinase activity

The isoprenylated membrane-associated RAS or RHOA proteins and the non-isoprenylated cytosolic forms were detected as previously described[20]. ERK1-2, AKT and RHOA kinases activity measurement details are reported in Supplemental Information.

Cell viability assay

Cell viability was evaluated by flow cytometry using with Annexin-V/Propidium Iodide (Ann-V/PI) staining with the MEBCYTO-Apoptosis Kit (MBL Medical and Biological Laboratories, Naka-ku Nagoya).

Statistical analysis

GraphPad Prism (version 6.01, San Diego, CA) was used to perform paired and unpaired t-test, and to calculatòe Pearson correlation coefficient. Results are expressed as mean ± SEM, unless otherwise specified. Statistical significance was defined as a p value <0.05. Combination analysis was performed using Compusyn software; combinations were considered synergistic when combination index (CI) was <1.

Results

HIF-1α is overexpressed in CLL cells from TP53^{dis} patients and in TP53 knockout lymphoma cell lines

Expression levels of HIF-1α protein were comparatively evaluated in HD CD19+ cells, and in CLL cells isolated from *TP53*^{dis} and *TP53*^{wt} samples. As expected, HD CD19+ B cells did not express HIF-1α at the baseline normoxic conditions (data not shown). By contrast, leukemic cells from CLL patients exhibited detectable cytosolic and nuclear HIF-1α protein

(Figure 1A). Interestingly, CLL cells from patients carrying *TP53* abnormalities (*TP53*^{dis} CLL cells) had significantly higher amounts of the cytosolic and nuclear fractions of HIF-1α subunit, as well as a higher *HIF-1A* mRNA levels, compared to CLL cells isolated from *TP53*^{wt} cases (*TP53*^{wt} CLL cells) (Figure 1 A-B). We evaluated an enlarged cohort of cases and observed that the association between the expression of HIF-1α and the *TP53* status was not influenced by the IGHV mutational status (Supplemental Figure S1). The transcriptional activity of HIF-1α, was evaluated through the expression of selected target genes[13,15,27]. We found a higher expression of *GLUT1* and *ENO1* in *TP53*^{dis} CLL cells, compared to *TP53*^{wt} sòamples (Figure 1 C-D). To corroborate the finding of an association between HIF-1α expression and *TP53* status we exploited cell line models. Interestingly, the expression of HIF-1α protein and mRNA was higher in *TP53*^{ko} Granta-519 and Séraphine lymphoma cell lines, compared to the p53^{wt} (Figure 1 E-F). In line with this finding, the expression *VEGF*, *GLUT1* and *ENO1* was also significantly higher in *TP53*^{ko} than in *TP53*^{wt} Granta-519 and Séraphine cell lines (Figure 1G).

To further investigate the link between *TP53* and HIF-1α, we performed a GSEA on previously published microarray data from tumour cells isolated from 7 *TP53*^{dis} and 13 *TP53*^{wt} cases (geocode GSE18971)[28]. Data of GSEA cases revealed that the *TP53* abnormalities were associated with an upregulation of a number of genes belonging to the "*GROSS_HYPOXIA_VIA_ELK3_AND_HIF1A_UP*" gene set (Figure 2A). The protein ELK3 participates in the transcriptional response to hypoxia and controls the expression of several regulators of HIF-1α stability[29]. Consistently, the baseline expression of ELK3 was higher in *TP53*^{dis} compared to *TP53*^{wt} CLL cells (Figure 2B).

Given its role HIF-1α regulation[12,30], we also compared pVHL expression in *TP53*^{dis} and *TP53*^{wt} samples. Notably, CLL cells from *TP53*^{dis} patients had reduced amounts of pVHL compared to *TP53*^{wt} patients, most likely being responsible of a better stabilization of the HIF-1α protein and a repression of its proteasomal degradation in *TP53*^{dis} cells (Figure

2C). As for HIF-1α expression, there were no differences between pVHL levels according to the IGHV mutational status (Supplemental Figure S2). These data suggest that *TP53* abnormalities lead to a reduced expression of pVHL and subsequently to an accumulation of HIF-1α protein.

Hypoxia and SC further increase HIF-1α expression in CLL cells from TP53^{dis} and TP53^{wt} patients

We next investigated whether microenvironmental signals, such as oxygen deprivation[12] and the interactions with SC[20], had differential effects on HIF-1α according to the *TP53* status of the leukemic cells, also in an attempt to better define the underlying molecular mechanisms. To this end, CLL cells were cultured for 48 hours in condition of hypoxia or in the presence of SC. Of note, *ex vivo* culture partially abrogated the *TP53*-related differential expression of HIF-1α observed at the baseline in freshly isolated CLL cells. In hypoxia, we observed a marked upregulation of the cytosolic and nuclear fractions of HIF-1α protein which was independent from the *TP53* status (Figure 3A) and was associated to a reduced expression of pVHL (Figure 3B), and to an activation of the PI3K/AKT and RAS/ERK1-2 pathways (Figures 3 C-F). Consistently, we observed that blocking concentration of pharmacologic agents inhibiting ERK1-2 (PD98059) and PI3K (LY294002) effectively counteracted the hypoxia-induced HIF-1α upregulation, independently from the *TP53* status (Figure 3G).

In line with previous data[20], we observed a marked upregulation of the cytosolic and nuclear amounts of the HIF-1α, when CLL cells were co-cultured with the SC (Figure 4A). SC-induced HIF-1α elevation was not associated to a reduced pVHL expression in leukemic cells (Figure 4B), whereas we observed an increased activation of RHOA/RHOA kinase (Figures 4 C-D), PI3K/AKT (Figure 4E), andò RAS/ERK1-2 (Figure 4F) signalling pathways. As a confirmation, we found that targeted inhibition of ERK1-2, PI3K and RHOA

kinase by blocking concentrations of pharmacologic agents (i.e. PD98059, LY294002 and Y27632, respectively) effective counteracted SC-induced HIF-1α upregulation (Figure 4G). The role of these pathways in modulating HIF-1α overexpression was corroborated by titration experiments showing that exposure of *TP53*^{dis} and *TP53*^{wt} CLL cells to increasing concentrations of PD98059, LY294002 and Y27632 induced a progressive reduction of the activity of the targeted kinases, which was associated to a dose-dependent decrease in HIF-1α levels (Supplemental Figure S3).

The selective HIF-1α inhibitor BAY87-2243 has anti-tumour activities in CLL

In line with the role of HIF-1α as a cells survival promoting factor[12], we found a positive correlation between the baseline levels of *HIF-1A* mRNA and the 48-hour viability of CLL cells during *in vitro* culture (Figure 5A). Consistently, the viability of leukemic cells isolated from samples characterized by baseline *HIF-1A* mRNA levels above the median value of the entire cohort (*HIF-1A*^{high}) was significantly higher than the viability of CLL cells displaying lower *HIF-1A* values (*HIF-1A*^{low}) (Figure 5B and Supplemental Figure S4). Based on these observations and on previous data reporting HIF-1α as a potential therapeutic target in CLL[17], we evaluated the anti-tumour effect of BAY87-2243, a selective inhibitor of HIF-1α. First, we observed that BAY87-2243 effectively inhibited HIF-1α protein expression at the cytosolic and nuclear level, both in *TP53*^{dis} and *TP53*^{wt} CLL cells (Figure 5C), also counteracting the HIF-1α upregulation exerted by hypoxia and SC (Figures 5 D-E). After 48 hours, BAY87-2243 determined a strong cytotoxic effect toward leukemic cells isolated from both patient subsets (Figure 5F and Supplemental Figure S5). Of note, the downregulation of HIF-1α was also evident at 24-hour exposure, when cell viability was still well preserved, thus confirming that it was determined by a targeted inhibitory effect rather than by a consequence of cell death (data not shown). BAY87-2243 exerted a cytotoxic effect also when *TP53*^{dis} and *TP53*^{wt} CLL cells were cultured for 48

hours in the presence of extrinsic signals inducing a further upregulation of baseline levels of HIF-1α, such as hypoxia (Figure 5G and Supplemental Figure S6) and co-culture with SC (Figure 5H and Supplemental Figure S7).

To further corroborate these data and the ability of BAY87-2243 to exert effective anti-tumour functions in CLL, we utilized a murine model derived from the transfer of Eμ-TCL1 leukemic cells into syngeneic mice[17]. In line with the results reported by Valsecchi et al.[17], showing that HIF-1α regulates the interaction of CLL cells with the bone marrow (BM) microenvironment, we observed that BAY87-2243 significantly reduced BM infiltration by leukemic cells, also inducing cytotoxicity in a consistent proportion of CLL cells (Figure 5 I-K). The anti-tumour effect observed with BAY87-2243 in the BM was not evident in the PB and spleen compartments (data not shown), suggesting that in a murine model of aggressive and rapidly growing CLL, HIF-1α may serve as a pro-survival factor especially for the leukemia reservoir residing in the BM.

In conclusion, our data indicate that HIF-1α is a pro-survival factor in CLL, which can be effectively targeted by the pharmacologic agent BAY87-2243, a specific inhibitor with potent anti-tumour effects both *in vitro* and *in vivo*.

BAY87-2243 restores fludarabine sensitivity of TP53^{dis} CLL cells and counteracts the protective effect of SC

We next examined whether BAY87-2243 was also effective in overcoming the intrinsic resistance to fludarabine of CLL cells from *TP53*^{dis} patients[9,31–33]. As expected, in our cohort, the normalized cell viability after 48-hour F-ara-A treatment was significantly higher in *TP53*^{dis} compared to *TP53*^{wt} CLL cells (Figure 6A). Consistently, we observed that CLL cells with a normalized cell viability ≥0.5, arbitrarily considered as *fludarabine-resistant*, were mostly *TP53*^{dis} and had a significantly higher baseline expression of *HIF-1A* mRNA compared to *fludarabine-sensitive* cells (i.e. normalized cell viability <0.5) (Figure 6B).

Interestingly, BAY87-2243 enhanced the cytotoxicity of fludarabine on *TP53*^{dis} CLL cells, as shown by the significant impairment of cell viability observed after combined treatment with BAY87-2243 + fludarabine compared to each compound used as a single agent (Figure 6C). The cytotoxic effect exerted by the combination was strongly synergistic (CI=0.17) on *TP53*^{dis} CLL cells and was also evident, although less remarkable, on *TP53*^{wt} CLL cells (Figure 6C and Supplemental Figure S8). Interestingly, we observed that combinations consisting of lower concentrations of BAY87-2243 + fludarabine were capable to induce significant reductions of the cell viability compared to each drug used as a single agent, and this effect was particularly evident in the *TP53*^{dis} CLL subset (Figure 6D). The cytotoxic activity of the combinations was also strongly synergistic as shown by data on CI (Supplemental Figure S9). Notably, the significantly higher cytotoxicity of the combination BAY87-2243 + fludarabine was maintained even when both *TP53*^{dis} and *TP53*^{wt} CLL cells were cultured under hypoxia (Supplemental Figures S10 A-B) or in the presence of SC (Supplemental Figures S10 C-D).

These results indicate that BAY87-2243 and fludarabine synergistically eliminate primary CLL cells, and that their effect was maintained even in the presence of HIF-1α inducing factors that recapitulate the BM niche microenvironment.

The combination of BAY87-2243 and ibrutinib exerts a synergistic cytotoxic effect on CLL cells

Previously reported data indicate that *TP53*-mutated CLL cells have a lower sensitivity to ibrutinib cytotoxicity *in vitro*[34] and that ibrutinib-induced apoptosis is significantly reduced in conditions of hypoxia[19]. Therefore, we hypothesized that the combination of a HIF-1α inhibitor and ibrutinib may represent a potentially attractive next step for patients carrying *TP53* abnormalities, who are characterized by constitutively higher levels of HIF-1α. Our results show that the combination of BAY87-2243 + ibrutinib determined a significant

impairment in the viability of *TP53*^{dis} and *TP53*^{wt} CLL cells, compared to each compound used as a single agent and was very strongly synergistic (Figure 7A and Supplemental Figure S11). Interestingly, similar effects were observed also with lower concentrations of both agents (Figure 7B and Supplemental Figure S12). Notably, the combination BAY87-2243 + ibrutinib exerted a significantly higher cytotoxic effect compared to each single compound even when CLL cells from both *TP53*^{dis} and *TP53*^{wt} samples were cultured in the presence of SC (Figure 7C).

Overall, these data demonstrate that BAY87-2243 exerts a compelling synergistic effect with ibrutinib, thus providing the rationale for future clinical translation.

Discussion

In this study, we investigated the expression and regulation of HIF-1α in *TP53*^{dis} CLL cells, and its potential role as a therapeutic target. We found that CLL cells carrying *TP53* abnormalities express significantly higher baseline levels of HIF-1α and have increased HIF-1α transcriptional activity compared to *TP53*^{wt} cells. Regardless of the *TP53* status, the resting levels of HIF-1α are susceptible to further upregulation by microenvironmental stimuli, such as hypoxia and SC. Our data show that HIF-1α is a suitable therapeutic target, whose inhibition induces a strong cytotoxic effect, capable also of reversing the *in vitro* fludarabine resistance of *TP53*^{dis} CLL cells and of exerting synergistic effects with ibrutinib.

Hypoxia has a detrimental role in the pathobiology of several solid and hematologic tumours[35,36]. The identification of new potential targets in CLL is certainly important for high-risk patients, for which an effective cure is still lacking, and in addition, the development of new therapies might be effective in a broader setting of B lymphoproliferative disorders.

It has been previously reported that HIF-1α levels vary considerably among CLL patients and that its overexpression is a predictor of a poor survival[17,37]. In line with observations made in solid tumours, where p53 promotes the ubiquitination and proteasomal degradation of the HIF-1α subunit in hypoxia[12,22], we postulated that abnormalities of the *TP53* gene might have an influence on the regulation of HIF-1α in CLL cells. To the best of our knowledge, this is the first study examining the differential expression and transcriptional activity of HIF-1α in patients with *TP53*-deficient CLL, also uncovering new mechanisms for HIF-1α modulation in leukemic cells. Our data show that the high-resting levels of HIF-1α detected in *TP53*^{dis} samples associate both to an increased transcription, as shown by the higher *HIF-1A* mRNA levels, and to a decreased degradation, as shown by the higher baseline expression of ELK3 and by the lower pVHL amounts.

We next investigated the cellular pathways implicated in HIF-1α regulation mediated by extrinsic factors. Hypoxia-induced HIF-1α upregulation is not only due to a reduced pVHL-mediated protein degradation, which is a well-known mechanism in condition of oxygen deprivation, but also to an increased activation of RAS/ERK1-2 and PI3K/AKT signalling pathways. By contrast, pVHL expression in leukemic cells is not affected by SC, which instead activate the RAS/ERK1-2, RHOA/RHOA kinase and PI3K/AKT intracellular pathways, thus leading to HIF-1α overexpression. These results endorse recent data that implicate a number of paracrine factors in the transcriptional and translational regulation of HIF-1α in different tumour models[38].

Previous data have suggested that HIF-1α targeting is a promising therapeutic strategy in CLL, potentially capable of synergizing with chemotherapeutic agents. The only HIF-1α inhibitor that has been preclinically tested in CLL is EZN-2208 - a topoisomerase I inhibitor that has also shown to downmodulate HIF-1α[17]. We therefore tested, BAY87-2243, a more selective HIF-1α inhibitor that has already shown *in vivo* anti-tumour efficacy in a lung tumour model, without any signs of toxicity[39]. Interestingly, BAY87-2243 demonstrated a

direct cytotoxicity towards leukemic cells isolated from CLL patients, and this effect was independent from the *TP53* status. As far as we know, this is the first evidence of the anti-tumour activity of BAY87-2243 in hematologic tumours and particularly in CLL.

Patients with CLL and *TP53* abnormalities are intrinsically resistant to fludarabine-based chemotherapy regimens[9,31–33,40,41]. Supported by our data demonstrating i) higher baseline levels of HIF-1α in *fludarabine-resistant* CLL cells and ii) a further upregulation of HIF-1α after exposure to hypoxia and SC, we investigated the ability of BAY87-2243 to overcome both intrinsic (i.e. *TP53*-related) and inducible (i.e. SC-induced) resistance to fludarabine. Our data show that BAY87-2243 potently synergizes with fludarabine *in vitro,* and that their combined cytotoxic effect was especially evident in *TP53*^{dis} samples. Interestingly, HIF-1α inhibition was also effective in overcoming the *TP53*-independent fludarabine-resistance induced by extrinsic factors recapitulating the BM microenvironment.

Since HIF-1α critically regulates the interactions of CLL cells with the BM stroma[17], the cytotoxic effects exerted by BAY87-2243 in culture systems mimicking the tumour niche could be in part the result of a perturbation of molecular circuits triggered by microenvironmental stimuli, which are implicated in cell survival and drug resistance. Data showing that hypoxia and SC induce HIF-1α overexpression support the hypothesis that, within the tumour niche, leukemic cells become highly dependent on its pro-survival effect. In line with this assumption, we found that treatment with BAY87-2243 induced a marked reduction of leukemic infiltration and a parallel increase in the proportion of apoptotic leukemic cells in the BM of a CLL transplantable model derived from the Eμ-TCL1 transgenic mice. Of note, the inhibition of HIF-1α may have beneficial effects also on the non-leukemic milieu. Recent data have shown that infiltration by CLL cells into BM could result in tissue-site hypoxia, causing i) increased expression of HIF-1α in hematopoietic progenitors, which leads to an impaired haematopoiesis and a reduced output of innate immune cells into the blood, and ii) impaired functions of different immune cells

subsets[19,42]. Overall, these evidences endorse the concept of HIF-1α inhibition as a very promising therapeutic strategy in CLL.

In the era of new targeted treatments, ibrutinib has determined a dramatic change in the therapeutic landscape and has become the standard of care for the majority of CLL patients[43–45]. However, i) ibrutinib is not suitable for all CLL patients and may have limited availability in several Countries, ii) complete responses are infrequent, and indefinite drug administration is usually needed to maintain a clinical response, and iii) the development of ibrutinib resistance in CLL cells has been demonstrated[46,47]. Even more importantly, *TP53*^{dis} CLL patients show a suboptimal long-term response to ibrutinib[48], and *TP53*-mutated CLL cells have a lower sensitivity to ibrutinib cytotoxicity *in vitro*[34]. Since our data show that *TP53*^{dis} samples are characterized by higher levels and function of HIF-1α, which is a crucial target to overcome the constitutive and inducible drug resistance of CLL cells, we hypothesized that the combination of BAY87-2243 and ibrutinib might be an appealing approach for *in vitro* testing. We found that dual targeting of HIF-1α alongside BTK function produces a synergistic cytotoxic activity towards primary CLL cells, also in the presence of *TP53* abnormalities, thus suggesting the possibility of improving ibrutinib efficacy through this novel therapeutic association.

Overall, our data indicate that HIF-1α is overexpressed in CLL cells, especially in the presence of *TP53* aberrations, and that is susceptible of further upregulation by microenvironmental stimuli. From the translational standpoint, the pharmacologic compound BAY87-2243, a selective inhibitor of HIF-1α, displays potent anti-tumour properties and warrants further pre-clinical evaluation in this disease setting, also in combination with other therapies. Indeed, on one hand the synergism of BAY87-2243 and fludarabine may provide the rationale for future clinical application in Countries with limited access to ibrutinib, particularly for the treatment of high-risk patients carrying *TP53* abnormalities. On the other hand, BAY87-2243 coupled with ibrutinib may offer a rational

combination to increase the proportion of minimal residual disease negative remissions, thus reducing the development of CLL clones with resistance mutations.

References

1. Hallek M, Fischer K, Fingerle-Rowson G, et al. Addition of rituximab to fludarabine and cyclophosphamide in patients with chronic lymphocytic leukaemia: a randomised, open-label, phase 3 trial. Lancet Lond Engl. 2010;376(9747):1164–1174.

2. Zenz T, Vollmer D, Trbusek M, et al. TP53 mutation profile in chronic lymphocytic leukemia: evidence for a disease specific profile from a comprehensive analysis of 268 mutations. Leukemia. 2010;24(12):2072–2079.

3. Parikh SA. Chronic lymphocytic leukemia treatment algorithm 2018. Blood Cancer J. 2018;8(10):93.

4. Sutton L-A, Rosenquist R. Deciphering the molecular landscape in chronic lymphocytic leukemia: time frame of disease evolution. Haematologica. 2015;100(1):7–16.

5. Zenz T, Eichhorst B, Busch R, et al. TP53 mutation and survival in chronic lymphocytic leukemia. J Clin Oncol. 2010;28(29):4473–4479.

6. Gonzalez D, Martinez P, Wade R, et al. Mutational status of the TP53 gene as a predictor of response and survival in patients with chronic lymphocytic leukemia: results from the LRF CLL4 trial. J Clin Oncol. 2011;29(16):2223–2229.

7. Campo E, Cymbalista F, Ghia P, et al. TP53 aberrations in chronic lymphocytic leukemia: an overview of the clinical implications of improved diagnostics. Haematologica. 2018;103(12):1956-1968.

8. Seiffert M, Dietrich S, Jethwa A, Glimm H, Lichter P, Zenz T. Exploiting biological diversity and genomic aberrations in chronic lymphocytic leukemia. Leuk Lymphoma. 2012;53(6):1023–1031.

9. Gaidano G, Rossi D. The mutational landscape of chronic lymphocytic leukemia and its impact on prognosis and treatment. Hematol Am Soc Hematol Educ Program. 2017;2017(1):329–337.

10. Thompson PA, Burger JA. Bruton's tyrosine kinase inhibitors: first and second generation agents for patients with Chronic Lymphocytic Leukemia (CLL). Expert Opin Investig Drugs. 2018;27(1):31–42.

11. O'Brien S, Furman RR, Coutre S, et al. Single-agent ibrutinib in treatment-naïve and relapsed/refractory chronic lymphocytic leukemia: a 5-year experience. Blood. 2018;131(17):1910–1919.

12. Masoud GN, Li W. HIF-1α pathway: role, regulation and intervention for cancer therapy. Acta Pharm Sin B. 2015;5(5):378–389.

13. Semenza GL. Targeting HIF-1 for cancer therapy. Nat Rev Cancer. 2003;3(10):721.

14. Singh D, Arora R, Kaur P, Singh B, Mannan R, Arora S. Overexpression of hypoxia-inducible factor and metabolic pathways: possible targets of cancer. Cell Biosci. 2017;762.

15. Semenza G. Signal transduction to hypoxia-inducible factor 1. Biochem Pharmacol. 2002;64(5–6):993–998.

16. Ghosh AK, Shanafelt TD, Cimmino A, et al. Aberrant regulation of pVHL levels by microRNA promotes the HIF/VEGF axis in CLL B cells. Blood. 2009;113(22):5568–5574.

17. Valsecchi R, Coltella N, Belloni D, et al. HIF-1α regulates the interaction of chronic lymphocytic leukemia cells with the tumor microenvironment. Blood. 2016;127(16):1987–1997.

18. Koczula KM, Ludwig C, Hayden R, et al. Metabolic plasticity in CLL: adaptation to the hypoxic niche. Leukemia. 2016;30(1):65–73.

19. Serra S, Vaisitti T, Audrito V, et al. Adenosine signaling mediates hypoxic responses in the chronic lymphocytic leukemia microenvironment. Blood Adv. 2016;1(1):47.

20. Rigoni M, Riganti C, Vitale C, et al. Simvastatin and downstream inhibitors circumvent constitutive and stromal cell-induced resistance to doxorubicin in IGHV unmutated CLL cells. Oncotarget. 2015;6(30):29833–29846.

21. Hientz K, Mohr A, Bhakta-Guha D, Efferth T. The role of p53 in cancer drug resistance and targeted chemotherapy. Oncotarget. 2016;8(5):8921–8946.

22. Amelio I, Melino G. The p53 family and the hypoxia-inducible factors (HIFs): determinants of cancer progression. Trends Biochem Sci. 2015;40(8):425–434.

23. Salnikow K, Costa M, Figg WD, Blagosklonny MV. Hyperinducibility of hypoxia-responsive genes without p53/p21-dependent checkpoint in aggressive prostate cancer. Cancer Res. 2000;60(20):5630–5634.

24. Hallek M, Cheson BD, Catovsky D, et al. Guidelines for the diagnosis and treatment of chronic lymphocytic leukemia: a report from the International Workshop on Chronic

Lymphocytic Leukemia updating the National Cancer Institute-Working Group 1996 guidelines. Blood. 2008;111(12):5446–5456.

25. Bomben R, Dal-Bo M, Benedetti D, et al. Expression of mutated IGHV3-23 genes in chronic lymphocytic leukemia identifies a disease subset with peculiar clinical and biological features. Clin Cancer Res. 2010;16(2):620–628.

26. Subramanian A, Tamayo P, Mootha VK, et al. Gene set enrichment analysis: a knowledge-based approach for interpreting genome-wide expression profiles. Proc Natl Acad Sci U S A. 2005;102(43):15545–15550.

27. Semenza GL, Jiang BH, Leung SW, et al. Hypoxia response elements in the aldolase A, enolase 1, and lactate dehydrogenase A gene promoters contain essential binding sites for hypoxia-inducible factor 1. J Biol Chem. 1996;271(51):32529–32537.

28. Dal Bo M, Pozzo F, Bomben R, et al. ARHGDIA, a mutant TP53-associated Rho GDP dissociation inhibitor, is over-expressed in gene expression profiles of TP53 disrupted chronic lymphocytic leukaemia cells. Br J Haematol. 2013;161(4):596–599.

29. Gross C, Dubois-Pot H, Wasylyk B. The ternary complex factor Net/Elk-3 participates in the transcriptional response to hypoxia and regulates HIF-1 alpha. Oncogene. 2008;27(9):1333–1341.

30. Liu W, Xin H, Eckert DT, Brown JA, Gnarra JR. Hypoxia and cell cycle regulation of the von Hippel-Lindau tumor suppressor. Oncogene. 2011;30(1):21–31.

31. Turgut B, Vural O, Pala FS, et al. 17p Deletion is associated with resistance of B-cell chronic lymphocytic leukemia cells to in vitro fludarabine-induced apoptosis. Leuk Lymphoma. 2007;48(2):311–320.

32. Dietrich S, Oleś M, Lu J, et al. Drug-perturbation-based stratification of blood cancer. J Clin Invest. 2018;128(1):427–445.

33. Nadeu F, Delgado J, Royo C, et al. Clinical impact of clonal and subclonal TP53, SF3B1, BIRC3, NOTCH1, and ATM mutations in chronic lymphocytic leukemia. Blood. 2016;127(17):2122–2130.

34. Guarini A, Peragine N, Messina M, et al. Unravelling the suboptimal response of TP53-mutated chronic lymphocytic leukaemia to ibrutinib. Br J Haematol. 2019;184(3):392-396.

35. Kim J-Y, Lee J-Y. Targeting Tumor Adaption to Chronic Hypoxia: Implications for Drug Resistance, and How It Can Be Overcome. Int J Mol Sci. 2017;18(9):1854.

36. Muz B, de la Puente P, Azab F, Luderer M, Azab AK. The role of hypoxia and exploitation of the hypoxic environment in hematologic malignancies. Mol Cancer Res. 2014;12(10):1347–1354.

37. Kontos CK, Papageorgiou SG, Diamantopoulos MA, et al. mRNA overexpression of the hypoxia inducible factor 1 alpha subunit gene (HIF1A): An independent predictor of poor overall survival in chronic lymphocytic leukemia. Leuk Res. 2017;53:65–73.

38. Kuschel A, Simon P, Tug S. Functional regulation of HIF-1α under normoxia--is there more than post-translational regulation? J Cell Physiol. 2012;227(2):514–524.

39. Ellinghaus P, Heisler I, Unterschemmann K, et al. BAY 87-2243, a highly potent and selective inhibitor of hypoxia-induced gene activation has antitumor activities by inhibition of mitochondrial complex I. Cancer Med. 2013;2(5):611–624.

40. Döhner H, Fischer K, Bentz M, et al. p53 gene deletion predicts for poor survival and non-response to therapy with purine analogs in chronic B-cell leukemias. Blood. 1995;85(6):1580–1589.

41. Zenz T, Häbe S, Denzel T, et al. Detailed analysis of p53 pathway defects in fludarabine-refractory chronic lymphocytic leukemia (CLL): dissecting the contribution of 17p deletion, TP53 mutation, p53-p21 dysfunction, and miR34a in a prospective clinical trial. Blood. 2009;114(13):2589–2597.

42. Manso BA, Zhang H, Mikkelson MG, et al. Bone marrow hematopoietic dysfunction in untreated chronic lymphocytic leukemia patients. Leukemia. 2019;33(3):638-652.

43. Eichhorst B, Robak T, Montserrat E, et al. appendix 6: Chronic lymphocytic leukaemia: eUpdate published online September 2016 (http://www.esmo.org/Guidelines/Haematological-Malignancies). Ann Oncol. 2016;27(suppl 5):v143–v144.

44. Eichhorst B, Robak T, Montserrat E, et al. Chronic lymphocytic leukaemia: ESMO Clinical Practice Guidelines for diagnosis, treatment and follow-up. Ann Oncol. 2015;26 Suppl 5:v78-84.

45. NCCN Guidelines Insights: Chronic Lymphocytic Leukemia/Small Lymphocytic Leukemia, Version 1.2017. http://www.jnccn.org/content/15/3/293.long (accessed February 11, 2018).

46. Woyach JA, Ruppert AS, Guinn D, et al. BTKC481S-Mediated Resistance to Ibrutinib in Chronic Lymphocytic Leukemia. J Clin Oncol. 2017;35(13):1437–1443.

47. Jones D, Woyach JA, Zhao W, et al. PLCG2 C2 domain mutations co-occur with BTK and PLCG2 resistance mutations in chronic lymphocytic leukemia undergoing ibrutinib treatment. Leukemia. 2017;31(7):1645–1647.

48. Byrd JC, Furman RR, Coutre SE, et al. Three-year follow-up of treatment-naïve and previously treated patients with CLL and SLL receiving single-agent ibrutinib. Blood. 2015;125(16):2497–2506.

Figure Legends

Figure 1. HIF-1α is overexpressed and more active in primary cells isolated from patients with CLL and in lymphoma cell lines carrying a *TP53* disruption

The expression of HIF-1α and HIF-1α target genes was measured in *TP53*^{dis} and *TP53*^{wt} CLL cells and in lymphoma *TP53*^{wt} and *TP53*^{ko} cell lines. **(A)** WB analysis for HIF-1α protein expression in freshly isolated *TP53*^{dis} and *TP53*^{wt} CLL cells. A representative blot is shown with relative Unique Patient Numbers (UPN) and cumulative band intensity data obtained from the analysis of 17 *TP53*^{wt} and 15 *TP53*^{dis} CLL patients. Box plots represent median value and 25%-75% percentiles, whiskers represent minimum and maximum values of band intensity for each group. **(B-D)** RT-PCR analysis of *HIF-1A,* and its target genes *GLUT1* and *ENO1* expression levels in *TP53*^{dis} and *TP53*^{wt} CLL cells. **(E)** WB analysis for HIF-1α protein expression in the *TP53*^{wt} and *TP53*^{ko} Granta-519 and Séraphine cell lines. A representative blot of 3 independent experiments is shown. **(F)** RT-PCR analysis of *HIF-1A* in the *TP53*^{wt} and *TP53*^{ko} Granta-519 and Séraphine cell lines. **(G)** RT-PCR analysis of *VEGF, GLUT1* and *ENO1* in the *TP53*^{wt} and *TP53*^{ko} Granta-519 and Séraphine cell lines showed a significantly higher expression level of all analysed genes in *TP53*^{ko} samples. In panels B, C and D box and whiskers plots represent median values and 25%-75% percentiles, whiskers represent minimum and maximum values for each group. In panels F and G, bar graphs represent mean results obtained from 3 experiments together with SEM. **** $p<0.0001$, *** $p<0.001$, ** $p<0.01$ and * $p<0.05$.

Figure 2. *TP53*^{dis} CLL cells show an upregulation of several genes involved in response to hypoxia and express reduced levels of pVHL. (**A)** GSEA on CLL cells from *TP53*^{dis} and *TP53*^{wt} patients. The plot of the Enrichment Score (ES) versus the gene list index and a portion of the corresponding heatmap highlighting the relative expression of gene members belonging to the **"**GROSS_HYPOXIA_VIA_ELK3_AND_HIF1A_UP"

gene set are depicted. 54 out of 126 genes from the gene set were significantly upregulated in the *TP53*^{dis} cohort of patients compared to the *TP53*^{wt} cohort. **(B)** WB for ELK3 baseline expression in *TP53*^{dis} and *TP53*^{wt} CLL cells. A representative blot is shown with relative UPN and cumulative band intensity data obtained from the analysis of 9 *TP53*^{wt} and 6 *TP53*^{dis} CLL patients. **(C)** WB for pVHL baseline expression in *TP53*^{dis} and *TP53*^{wt} CLL cells. A representative blot is shown with relative UPN and cumulative band intensity data obtained from the analysis of 15 *TP53*^{wt} and 12 *TP53*^{dis} CLL patients. Box plots represent median value and 25%-75% percentiles, whiskers represent minimum and maximum values of band intensity for each group. **** $p<0.0001$, and *$p<0.05$.

Figure 3. Hypoxia further increases HIF-1α expression in *TP53*^{dis} and *TP53*^{wt} CLL cells via the PI3K/AKT and RAS/ERK1-2 signalling pathways.

Primary CLL cells were cultured for 48 hours under normoxic and hypoxic conditions. **(A, B)** WB analyses detected a higher amount of cytosolic and nuclear HIF-1α and lower amount of pVHL in *TP53*^{dis} and *TP53*^{wt} CLL cells cultured in hypoxia (H) compared to normoxia (N). **(C, D)** Immuno-enzymatic measurement showed that RHOA-GTP and RHOA kinase activities were unaffected by hypoxia. **(E, F)** WB analyses for AKT, RAS and ERK1-2. *TP53*^{dis} and *TP53*^{wt} CLL cells had higher expression of the active form of AKT [p(Ser 473)AKT], RAS (RAS-GTP) and ERK1-2 [p(Thr202/Tyr204, Thr185/Tyr187]ERK1-2) in hypoxia compared to normoxia. **(G)** WB analyses for HIF-1α. The targeting of ERK1-2 with 10 μM PD98059 (PD) and of PI3K with 10 μM LY294002 (LY) reduced HIF-1α expression in CLL cells, both in hypoxia and normoxia, and independently from the *TP53* status. In panel A, results are from 2 representative cases of 7 for *TP53*^{wt} patients and 2 representative cases of 5 for *TP53*^{dis} patients. Representative blots are shown with relative UPN and cumulative band intensity data. Box plots represent median values and 25%-75% percentiles, whiskers represent minimum and maximum values of band intensity for

each group. In panels B, E and F results are from 1 representative experiment of 4 for *TP53*^{wt} patients and 1 representative experiment of 3 for *TP53*^{dis} patients. Bar graphs represent mean values together with SEM. In panels C and D, multiple line graphs represent individual data values for the same sample in each condition. In panel G results are from 1 representative experiment of 3 for *TP53*^{wt} patients and 1 representative experiment of 3 for *TP53*^{dis} patients. Vertical lines have been inserted to indicate repositioned gel lanes. **** p<0.0001, ** p<0.01 and *p<0.05.

Figure 4. SC increase HIF-1α expression in *TP53*^{dis} and *TP53*^{wt} CLL cells via PI3K/AKT, RAS/ERK1-2 and RHOA/RHOA kinase signalling pathways.

Primary CLL cells were cultured for 48 hours in the presence and in absence of M2-10B4 SC. **(A, B)** WB analyses for HIF-1α and pVHL. SC upregulated the cytosolic and nuclear expression of HIF-1α but did not affect pVHL expression in *TP53*^{dis} and *TP53*^{wt} CLL cells. **(C, D)** Immuno-enzymatic measurement showed that the co-culture with SC increased RHOA-GTP and RHOA kinase activities in *TP53*^{dis} and *TP53*^{wt} CLL cells. **(E, F)** WB analyses for AKT, RAS and ERK1-2. Higher amount of the active form of AKT [p(Ser 473)AKT], RAS (RAS-GTP) and ERK1-2 [p(Thr202/Tyr204, Thr185/Tyr187)ERK1-2] were detectable in both *TP53*^{wt} and *TP53*^{dis} CLL cells cultured with SC. **(G)** WB analyses for HIF-1α. The targeting of ERK1-2 with 10 μM PD98059 (PD), 10 μM Y27632 (Y276) and of PI3K with 10 μM LY294002 (LY) reduced HIF-1α expression in CLL cells, both in presence and in the absence of SC, regardless of the *TP53* status. In panel A, results are from 2 representative cases of 10 for *TP53*^{wt} patients and 2 representative cases of 4 for *TP53*^{dis} patients. Representative blots are shown, together with UPN and cumulative band intensity data. Box plots represent median values and 25%-75% percentiles, whiskers represent minimum and maximum values of band intensity for each group. In panels B and G, results are from 1 representative experiment of 3 for *TP53*^{wt} patients and 1 representative experiment of 3 for *TP53*^{dis} patients. In panels C and D, multiple line graphs

represent individual data values for the same sample in each condition. In panels E and F, results are from 1 representative experiment of 5 for *TP53*^{wt} patients and 1 representative experiment of 4 for *TP53*^{dis} patients. Bar graphs represent mean values together with SEM. Vertical lines have been inserted to indicate repositioned gel lanes. **** p<0.0001, *** p<0.001, ** p<0.01 and *p<0.05.

Figure 5. HIF-1α promotes CLL cells survival and its inhibition exerts a direct cytotoxicity, also in the presence of HIF-1α inducing microenvironmental stimuli. (A) Correlation of *HIF-1A* gene expression and 48-hour cell viability of CLL cells as determined by Annexin V/propidium iodide assay. **(B)** The median value of *HIF-1A* mRNA expression of a cohort of 25 CLL samples was selected as the cut-off to identify *HIF-1A*^{high} and *HIF-1A*^{low} CLL cells. *HIF-1A*^{high} showed significantly higher 48-hour cell viability compared to *HIF-1A*^{low} CLL cells. **(C)** WB analyses for HIF-1α. The exposure to 1 μM BAY87-2243 (BAY) for 48 hours reduced the cytosolic and nuclear amount of HIF-1α in CLL cells isolated from both *TP53*^{wt} and *TP53*^{dis} patient subsets. A representative blot is shown, together with UPN and cumulative band intensity data obtained from the analysis of 14 *TP53*^{wt} and 4 *TP53*^{dis} CLL patients. Box plots represent median value and 25%-75% percentiles, whiskers represent minimum and maximum values of band intensity for each group. **(D, E)** Primary CLL cells were exposed to 1 μM BAY for 48 hours under normoxic and hypoxic conditions, in the absence and in presence of M2-10B4 SC, and evaluated for HIF-1α expression by WB. BAY87-2243 was able to lower HIF-1α expression in CLL cultured in normoxic and hypoxic conditions, and in the absence or presence of SC, independently from the *TP53* status. **(F-H)** Cell viability of *TP53*^{dis} and *TP53*^{wt} CLL cells exposed for 48 hours to 1 μM BAY87-2243, under normoxia and hypoxia, or in co-culture with SC. The treatment with BAY87-2243 determined a significant decrease in the viability of *TP53*^{wt} and *TP53*^{dis} CLL cells, compared to untreated controls, both in normoxia and

hypoxia. After exposure to SC, BAY87-2243 significantly reduced the viability of *TP53*^{dis} and *TP53*^{wt} CLL cells, not completely overcoming the SC protective effect. In blot representations, vertical lines have been inserted to indicate repositioned gel lanes. **(I)** Scheme of the *in vivo* experiment with mice transplanted with the Eμ-TCL1-derived leukemia. **(J)** Percentage of leukemic cells (CD19+) in the BM of mice transplanted with the Eμ-TCL1-derived leukemia, treated with BAY87-2243, and euthanized as in panel I. **(K)** Percentage of AnnV leukemic cells (CD19+) in the BM of mice transplanted with Eμ-TCL1-derived leukemia, treated with BAY87-4432, and euthanized as in panel **I**. In panel A data are represented by a scatter plot. In panels J and K data are represented as bee-swarm plots. In panel B box and whiskers plots represent median values and 25%-75% percentiles, whiskers represent minimum and maximum values for each group. In panel D, results are from 1 representative experiment of 3 for *TP53*^{wt} patients and 1 representative experiment of 3 for *TP53*^{dis} patients. In panel E, results are from 1 representative experiment of 7 for *TP53*^{wt} patients and 1 representative experiment of 4 for *TP53*^{dis} patients. In panels F, G and H box and whiskers plots represent median values and 25%-75% percentiles, whiskers represent minimum and maximum values for each group, together with all points. **** $p<0.0001$, *** $p<0.001$, ** $p<0.01$ and * $p<0.05$.

Figure 6. *HIF-1A* mRNA is overexpressed in *fludarabine-resistant* CLL cells and HIF-1α inhibition is capable of restoring fludarabine sensitivity. (A) Normalized cell viability (i.e. the ratio between the percentage of AnnV/PI negative CLL cells cultured in the presence of F-ara-A and the percentage of AnnV/PI negative CLL cells left untreated) of *TP53*^{dis} and *TP53*^{wt} CLL cells exposed for 48 hours to 10 μM F-ara-A. **(B)** A normalized cell viability of 0.5 was selected as the cut-off value to identify *fludarabine-resistant* (i.e. normalized cell viability ≥0.5) and *fludarabine-sensitive* (i.e. normalized cell viability <0.5) CLL cells. *Fludarabine-resistant* CLL cells showed significantly higher baseline levels of

HIF-1A mRNA compared to *fludarabine-sensitive*. Eight out of 10 (80%) *fludarabine-resistant* samples derived from *TP53*^{dis} patients, and 13 out of 14 (93%) *fludarabine-sensitive* samples derived from *TP53*^{wt} patients. **(C)** Normalized cell viability of *TP53*^{dis} and *TP53*^{wt} CLL cells exposed for 48 hours to 1 μM BAY87-2243 (BAY) and/or 10 μM F-ara-A. The combination BAY87-2243 + F-ara-A (striped pattern) determined a significant decrease in the viability of *TP53*^{wt} and *TP53*^{dis} CLL cells, compared to each compound used as single agent and to untreated controls. **(D)** Heatmaps showing normalized viability after 48-hour treatment with BAY87-2243 + fludarabine as single agents or in combination, used at different concentrations. Asterisks indicate the combinations which determined a significant reduction in cell viability compared to each single agent, at the corresponding concentration. In panels A and C, box plots represents median values and 25%-75% percentiles, whiskers represent minimum and maximum values for each group, together with all points. In panel B data are represented as bee-swarm plot. **** $p<0.0001$, *** $p<0.001$, ** $p<0.01$ and *$p<0.05$.

Figure 7. BAY87-2243 plus ibrutinib combinations exert synergistic cytotoxic effects and is effective in impairing CLL cells viability in the presence of SC. (**A**) Normalized 48-hour viability of *TP53*^{dis} and *TP53*^{wt} CLL cells exposed to 1 μM BAY87-2243 (BAY) and 10 μM ibrutinib, used as single agents or in combination (striped pattern). Box plots represent median value and 25%-75% percentiles, whiskers represent minimum and maximum values for each group, together with all points. (**B**) Heatmaps showing normalized viability after 48-hour treatment with BAY87-2243 + ibrutinib as single agents or in combination, used at different concentrations. Asterisks indicate the combinations which determined a significant reduction in cell viability compared to each single agent, at the corresponding concentration. (**C**) Normalized 48-hour viability of *TP53*^{dis} and *TP53*^{wt} CLL cells exposed to 1 μM BAY87-2243 (BAY) and 10 μM ibrutinib, used as single agents

or in combination (striped pattern), in co-culture with M2-10B4 SC. Box plots represent median value and 25%-75% percentiles, whiskers represent minimum and maximum values for each group, together with all points. *** $p<0.001$, ** $p<0.01$ and *$p<0.05$.

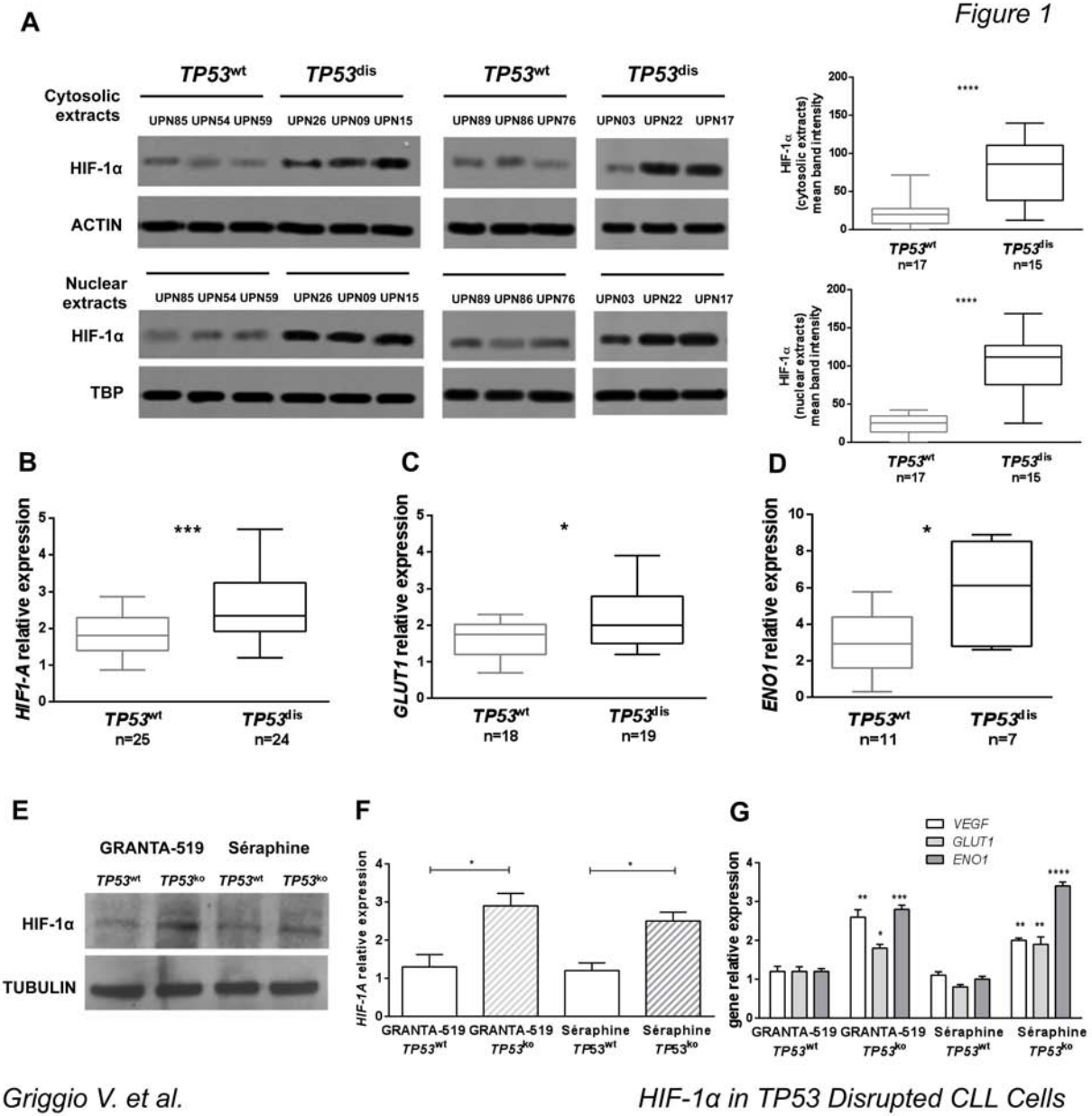
A
TP53wt
TP53dis
TP53wt
TP53dis
Cytosolic extracts
UPN85 UPN54 UPN59
UPN26 UPN09 UPN15
UPN89 UPN86 UPN76
UPN03 UPN22 UPN17
HIF-1α
ACTIN
Nuclear extracts
UPN85 UPN54 UPN59
UPN26 UPN09 UPN15
UPN89 UPN86 UPN76
UPN03 UPN22 UPN17
HIF-1α
TBP
HIF-1α (cytosolic extracts) mean band intensity
****
TP53wt n=17
TP53dis n=15
HIF-1α (nuclear extracts) mean band intensity
****
TP53wt n=17
TP53dis n=15
B
HIF1-A relative expression
***
TP53wt n=25
TP53dis n=24
C
GLUT1 relative expression
*
TP53wt n=18
TP53dis n=19
D
ENO1 relative expression
*
TP53wt n=11
TP53dis n=7
E
GRANTA-519
Séraphine
TP53wt
TP53ko
TP53wt
TP53ko
HIF-1α
TUBULIN
F
HIF-1A relative expression
GRANTA-519 TP53wt
GRANTA-519 TP53ko
Séraphine TP53wt
Séraphine TP53ko
G
VEGF
GLUT1
ENO1
gene relative expression
GRANTA-519 TP53wt
GRANTA-519 TP53ko
Séraphine TP53wt
Séraphine TP53ko

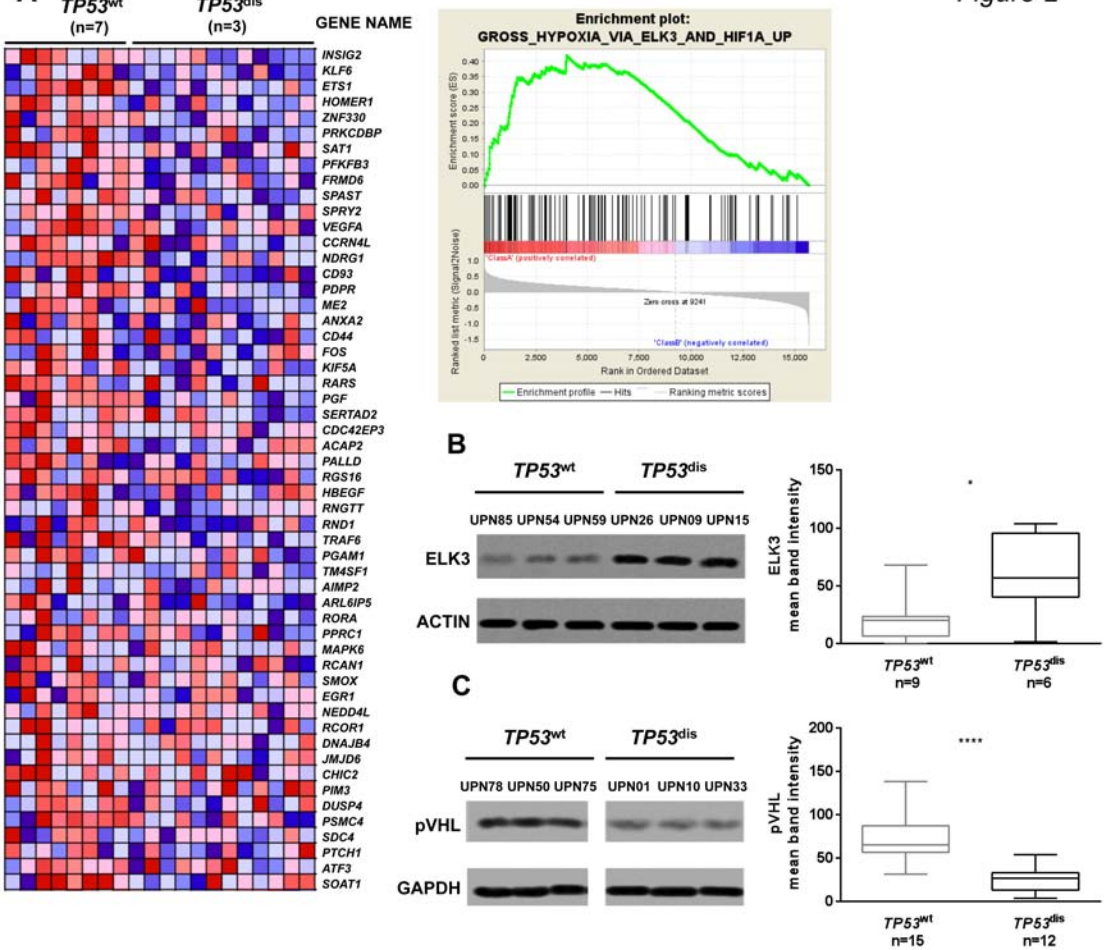
A
TP53wt (n=7)
TP53dis (n=3)
GENE NAME
INSIG2
KLF6
ETS1
HOMER1
ZNF330
PRKCDBP
SAT1
PFKFB3
FRMD6
SPAST
SPRY2
VEGFA
CCRN4L
NDRG1
CD93
PDPR
ME2
ANXA2
CD44
FOS
KIF5A
RARS
PGF
SERTAD2
CDC42EP3
ACAP2
PALLD
RGS16
HBEGF
RNGTT
RND1
TRAF6
PGAM1
TM4SF1
AIMP2
ARL6IP5
RORA
PPRC1
MAPK6
RCAN1
SMOX
EGR1
NEDD4L
RCOR1
DNAJB4
JMJD6
CHIC2
PIM3
DUSP4
PSMC4
SDC4
PTCH1
ATF3
SOAT1
Enrichment plot:
GROSS_HYPOXIA_VIA_ELK3_AND_HIF1A_UP
Enrichment score (ES)
Ranked list metric (Signal2Noise)
'ClassA' (positively correlated)
Zero cross at 9241
'ClassB' (negatively correlated)
Rank in Ordered Dataset
Enrichment profile
Hits
Ranking metric scores
B
TP53wt
TP53dis
UPN85 UPN54 UPN59 UPN26 UPN09 UPN15
ELK3
ACTIN
ELK3 mean band intensity
TP53wt n=9
TP53dis n=6
C
TP53wt
TP53dis
UPN78 UPN50 UPN75 UPN01 UPN10 UPN33
pVHL
GAPDH
pVHL mean band intensity
TP53wt n=15
TP53dis n=12

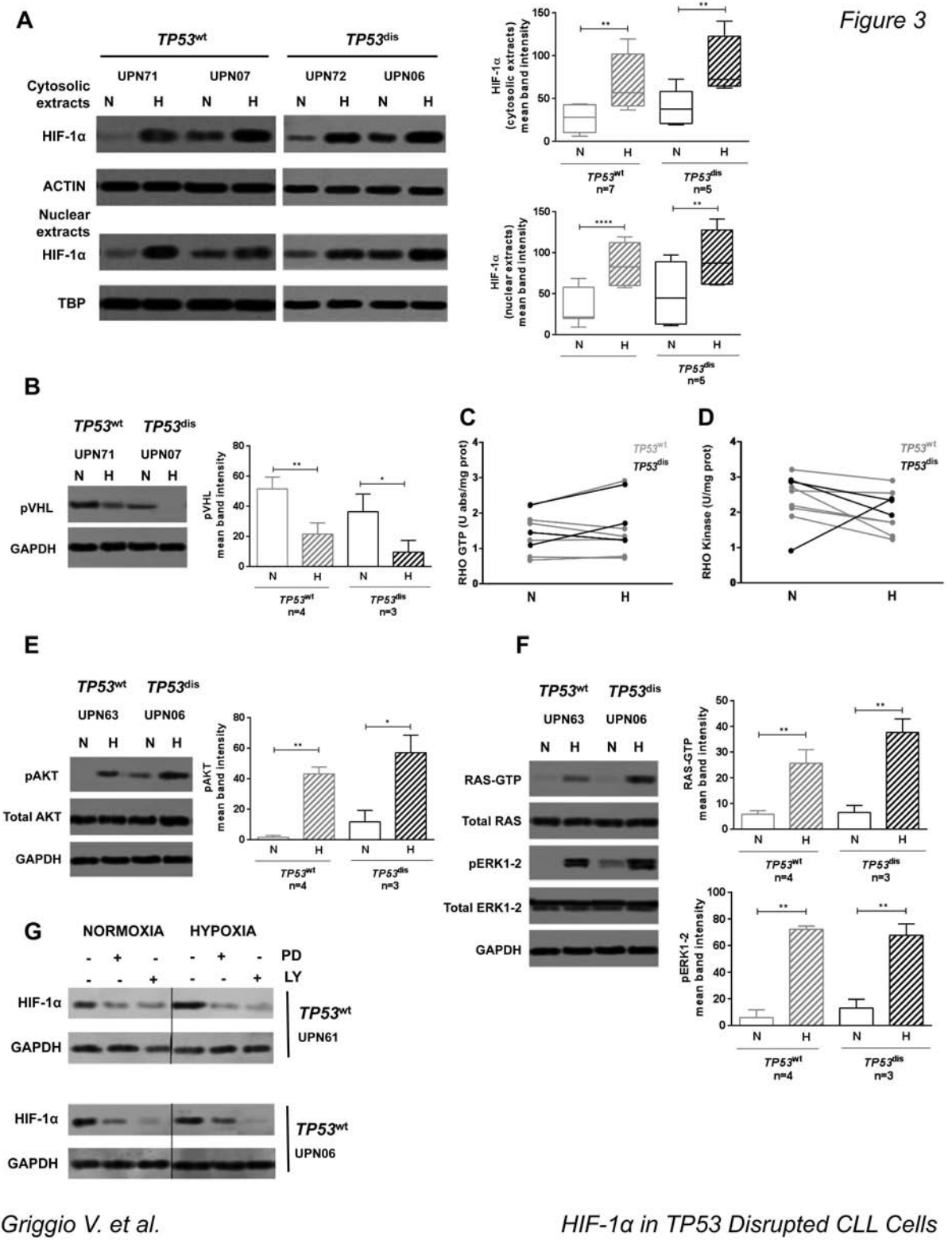
A
TP53wt
TP53dis
UPN71
UPN07
UPN72
UPN06
Cytosolic extracts
N H N H N H N H
HIF-1α
ACTIN
Nuclear extracts
HIF-1α
TBP
HIF-1α (cytosolic extracts) mean band intensity
TP53wt n=7
TP53dis n=5
HIF-1α (nuclear extracts) mean band intensity
TP53dis n=5
B
TP53wt
TP53dis
UPN71
UPN07
pVHL
GAPDH
pVHL mean band intensity
TP53wt n=4
TP53dis n=3
C
RHO GTP (U abs/mg prot)
TP53wt
TP53dis
D
RHO Kinase (U/mg prot)
TP53wt
TP53dis
E
TP53wt
TP53dis
UPN63
UPN06
pAKT
Total AKT
GAPDH
pAKT mean band intensity
TP53wt n=4
TP53dis n=3
F
TP53wt
TP53dis
UPN63
UPN06
RAS-GTP
Total RAS
pERK1-2
Total ERK1-2
GAPDH
RAS-GTP mean band intensity
TP53wt n=4
TP53dis n=3
pERK1-2 mean band intensity
TP53wt n=4
TP53dis n=3
G
NORMOXIA
HYPOXIA
PD
LY
HIF-1α
GAPDH
TP53wt
UPN61
HIF-1α
GAPDH
TP53wt
UPN06

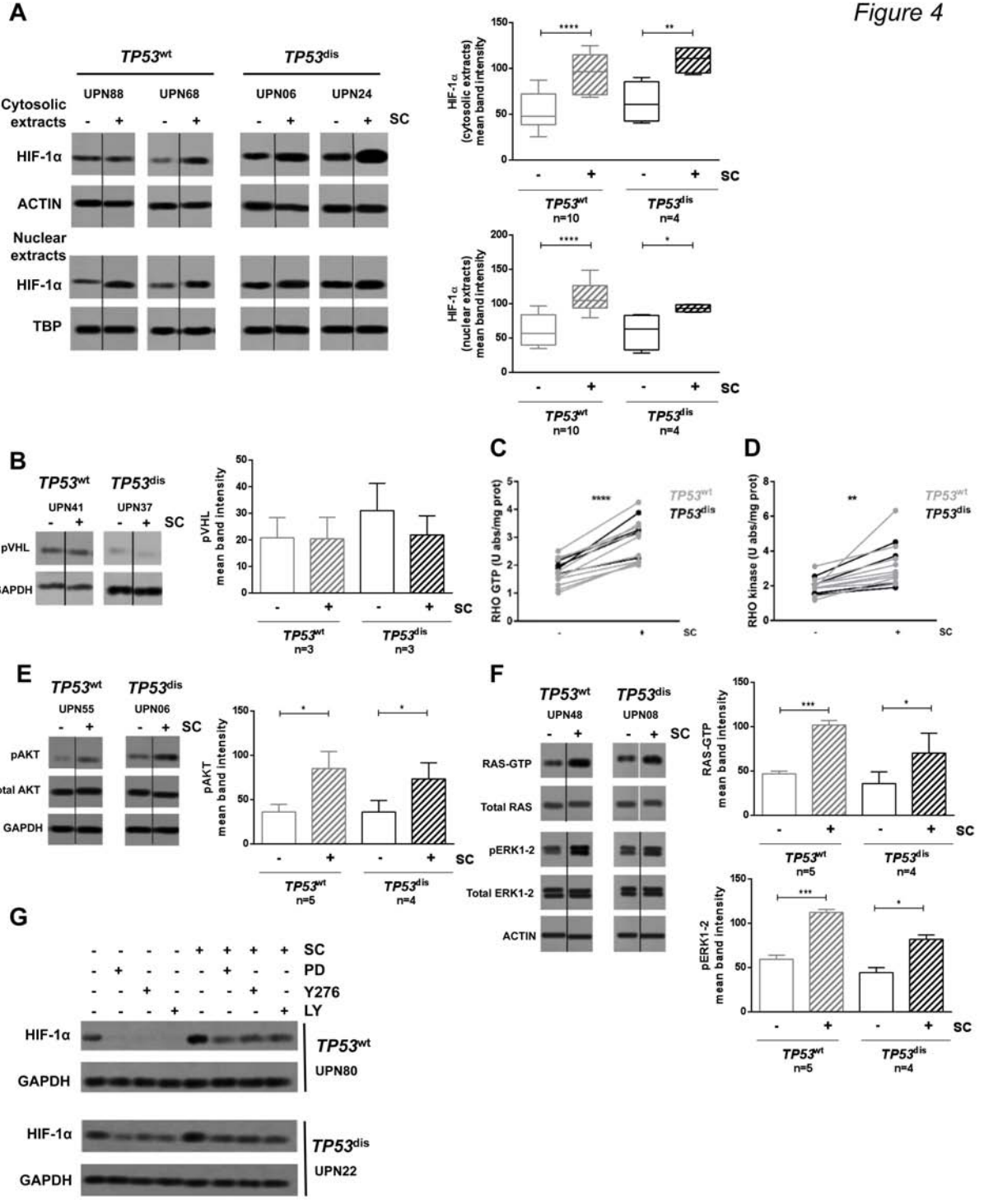
A
TP53wt
TP53dis
UPN88
UPN68
UPN06
UPN24
Cytosolic extracts
SC
HIF-1α
ACTIN
Nuclear extracts
HIF-1α
TBP
HIF-1α (cytosolic extracts) mean band intensity
HIF-1α (nuclear extracts) mean band intensity
TP53wt n=10
TP53dis n=4
B
UPN41
UPN37
pVHL
GAPDH
pVHL mean band intensity
TP53wt n=3
TP53dis n=3
C
RHO GTP (U abs/mg prot)
D
RHO kinase (U abs/mg prot)
E
UPN55
UPN06
pAKT
Total AKT
GAPDH
pAKT mean band intensity
TP53wt n=5
TP53dis n=4
F
UPN48
UPN08
RAS-GTP
Total RAS
pERK1-2
Total ERK1-2
ACTIN
RAS-GTP mean band intensity
pERK1-2 mean band intensity
G
PD
Y276
LY
UPN80
UPN22

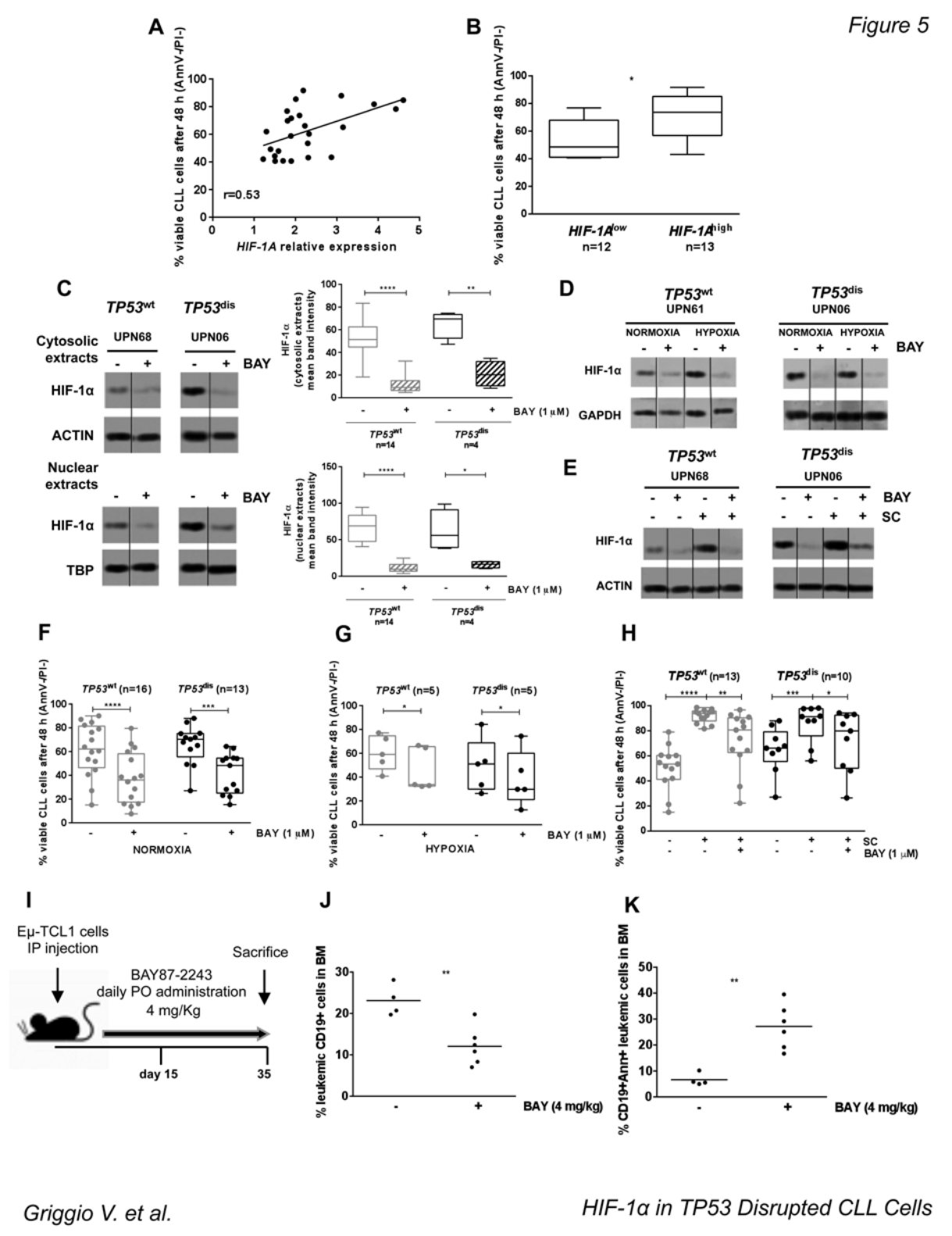
A
% viable CLL cells after 48 h (AnnV-/PI-)
r=0.53
HIF-1A relative expression
B
% viable CLL cells after 48 h (AnnV-/PI-)
HIF-1A low n=12
HIF-1A high n=13
C
TP53wt
TP53dis
Cytosolic extracts
UPN68
UPN06
BAY
HIF-1α
ACTIN
Nuclear extracts
TBP
HIF-1α (cytosolic extracts) mean band intensity
HIF-1α (nuclear extracts) mean band intensity
BAY (1 μM)
TP53wt n=14
TP53dis n=4
D
TP53wt UPN61
TP53dis UPN06
NORMOXIA
HYPOXIA
BAY
HIF-1α
GAPDH
E
TP53wt UPN68
TP53dis UPN06
BAY
SC
HIF-1α
ACTIN
F
% viable CLL cells after 48 h (AnnV-/PI-)
TP53wt (n=16)
TP53dis (n=13)
BAY (1 μM)
NORMOXIA
G
TP53wt (n=5)
TP53dis (n=5)
BAY (1 μM)
HYPOXIA
H
TP53wt (n=13)
TP53dis (n=10)
SC
BAY (1 μM)
I
Eμ-TCL1 cells IP injection
Sacrifice
BAY87-2243 daily PO administration 4 mg/Kg
day 15
35
J
% leukemic CD19+ cells in BM
BAY (4 mg/kg)
K
% CD19+Ann+ leukemic cells in BM
BAY (4 mg/kg)

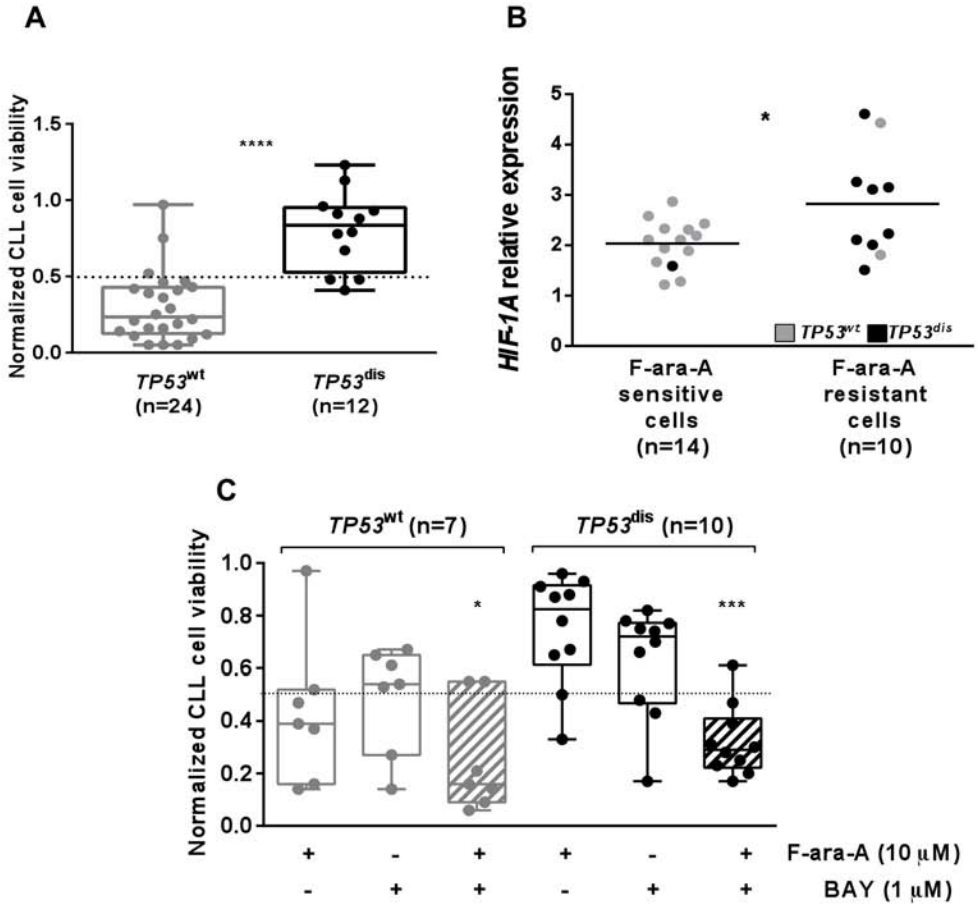

D

F-ara-A (μM)	TP53wt					TP53dis				
BAY (μM)	CTRL	0.01	0.1	1	10	CTRL	0.01	0.1	1	10
CTRL	1	0,93	0,86	0,45	0,38	1	1,00	1,00	0,79	0,65
0.01	0,87	0,88	0,90	0,44	0,33	0,96	1,00	0,95	0,79	0,53
0.1	0,78	0,73	0,71	0,44	0,34	0,80	0,86	0,71	0,60**	0,39***
0.5	0,7	0,66	0,71	0,41	0,31	0,84	0,77	0,85	0,70	0,44
1	0,63	0,67	0,61	0,45	0,27	0,74	0,86	0,70 *	0,54**	0,33***

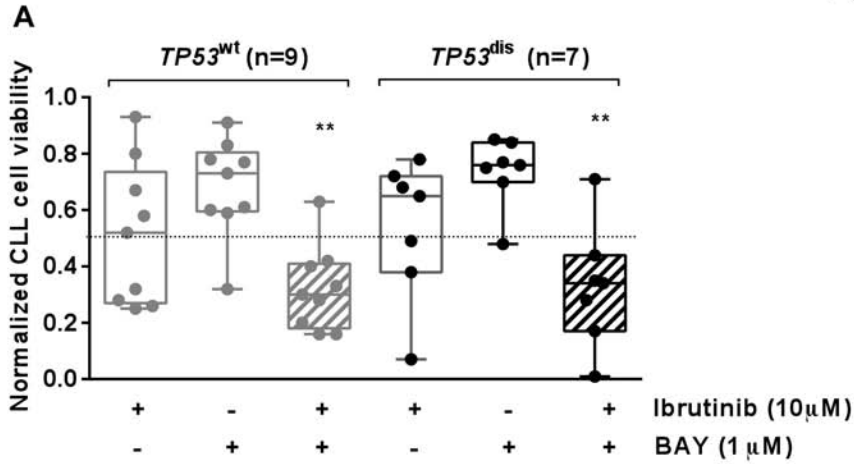

B

Ibrutinib (μM) / BAY (μM)	TP53wt CTRL	0.01	0.1	1	10	TP53dis CTRL	0.01	0.1	1	10
CTRL	1	0,86	0,86	0,79	0,55	1	0,98	0,82	0,79	0,54
0.01	0,87	0,70 *	0,70 **	0,65	0,48 *	0,96	0,84	0,73**	0,65 *	0,43**
0.1	0,78	0,58 *	0,61***	0,50***	0,37**	0,8	0,77	0,60**	0,59**	0,35**
0.5	0,7	0,60	0,53 *	0,48	0,39	0,84	0,66	0,67	0,73	0,41
1	0,63	0,56	0,53	0,56	0,33**	0,74	0,64	0,51***	0,52 *	0,33**

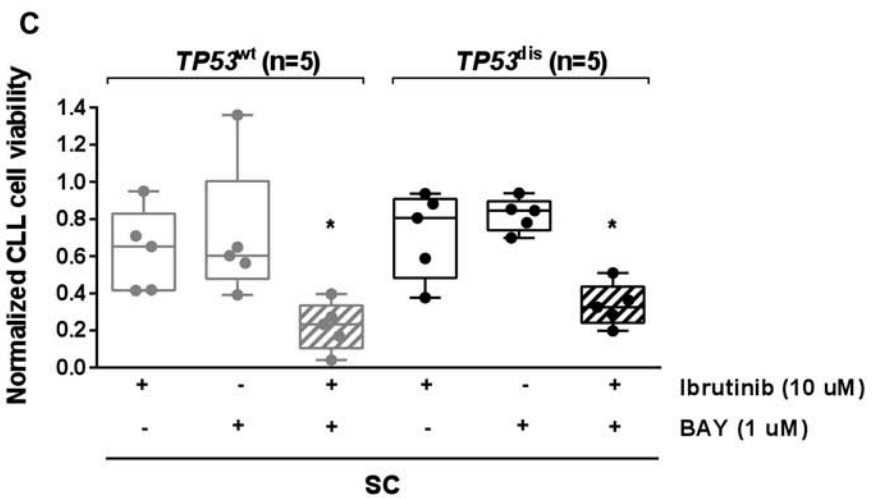

Supplemental Information

Article title: HIF-1α is overexpressed in leukemic cells from *TP53*-disrupted patients and is a promising therapeutic target in CLL

Running Head: HIF-1α in *TP53*-disrupted CLL Cells

Authors: Valentina Griggio[1,2], Candida Vitale[1,2], Maria Todaro[1,2], Chiara Riganti[3], Joanna Kopecka[3], Chiara Salvetti[1,2], Riccardo Bomben[4], Michele Dal Bo[4], Daniela Magliulo[5], Davide Rossi[6], Gabriele Pozzato[7], Lisa Bonello[2], Monia Marchetti[8], Paola Omedè[1], Ahad Ahmed Kodipad[9], Luca Laurenti[10], Giovanni Del Poeta[11], Francesca Romana Mauro[12]; Rosa Bernardi[5], Thorsten Zenz[13], Valter Gattei[4], Gianluca Gaidano[9], Robin Foà[12], Massimo Massaia[14], Mario Boccadoro[1,2] and Marta Coscia[1,2]

Affiliations:

[1]Division of Hematology, University of Torino, A.O.U. Città della Salute e della Scienza di Torino, Turin, Italy

[2]Department of Molecular Biotechnology and Health Sciences, University of Torino, Torino, Italy

[3]Department of Oncology, University of Torino, Turin, Italy

[4]Clinical and Experimental Onco-Hematology Unit, CRO Aviano National Cancer Institute, Aviano, Italy

[5]Division of Experimental Oncology, IRCCS San Raffaele Scientific Institute, Milan, Italy;

[6]Department of Hematology, Oncology Institute of Southern Switzerland and Institute of Oncology Research, Bellinzona, Switzerland

[7]Department of Internal Medicine and Hematology, Maggiore General Hospital, University of Trieste, Trieste, Italy

[8]Hematology Day Service, Oncology SOC, Hospital Cardinal Massaia, Asti, Italy

[9]Division of Hematology, Department of Translational Medicine, University of Eastern Piedmont, Novara, Italy

[10]Fondazione Policlinico Universitario Agostino Gemelli, Rome, Italy

[11]Division of Hematology, S. Eugenio Hospital and University of Tor Vergata, Rome, Italy

[12]Hematology, Department of Translational and Precision Medicine, Sapienza University, Policlinico Umberto I, Rome, Italy

[13]Department of Medical Oncology and Hematology, University Hospital and University of Zurich, Zurich, Switzerland

[14]Hematology Unit, ASO Santa Croce e Carle, Cuneo, Italy

V.Griggio and C.V. contributed equally to this study.

Supplemental Methods

Cells preparation and culture

PBMC were separated using Ficoll-Hypaque (Sigma-Aldrich) and stained with anti-CD19 PerCP Vio700 and anti-CD5-APC antibodies (Miltenyi Biotec, Bologna, Italy). When the CD19+/CD5+ cells were < 90%, CLL cells were purified by negative selection and cultured in RPMI-1640 medium with 10% of fetal bovine serum (FBS) and penicillin/streptomycin. B lymphocytes from healthy donors were purified by positive selection using anti-CD19 micro beads (Miltenyi Biotec). Del(17p) was assessed by *fluorescence in situ hybridization* and the presence of *TP53* gene mutations was evaluated by Sanger sequencing. Immunoglobulin heavy chain variable region gene (IGHV) mutational status was assessed as already described[1]. Cell lines used in the experiments (i.e. Séraphine, Granta-519 and M2-10B4) were maintained in RPMI-1640 or DMEM medium with 10% fetal bovine serum, glutamine and antibiotics at 37 °C, 5% CO_2. A humidified hypoxia incubator chamber was used for hypoxic cultures.

Antibodies used for flow cytometry

Two- and three-color flow cytometry was performed with FACSCalibur and CELLQuest software (Becton Dickinson, Mountain View, CA) and with BD Accuri C6 flow cytometer (BD Bioscences). Data were analyzed with FlowJo software (Tree Star, Inc, Ashland, OR). Antibodies used for flow cytometry were: anti-CD19-PE (BD Biosciences, San José, CA), anti-CD19-PerCP Vio700 (Miltenyi Biotec), anti-CD5-APC (Miltenyi Biotec).

Western blot analysis

Cytosolic and nuclear protein extracts were obtained using the Nuclear Extract Kit (Active Motif, La Hulpe) following the manufacturer's instructions. Lysates were resolved by SDS-PAGE and transferred to nitrocellulose membranes (Bio-Rad, Hercules, CA). The following antibodies were used: anti-HIF-1α (BD Biosciences, San José, CA), anti-ELK3

(Sigma Aldrich); anti-pVHL (EuroClone Spa, Milano); anti p(Thr202/Tyr204, Thr185/Tyr187)-ERK1–2 (Millipore, Bedford, MA); anti-ERK1-2 (Millipore); anti-RAS (Millipore); anti-RHOA (Santa Cruz Biotechnology Inc., Santa Cruz, CA) antibody anti-p(Ser 473)AKT (Millipore); anti-AKT (Millipore); anti-ACTIN (Sigma Aldrich), anti-GAPDH, anti-TUBULIN and anti-TATA-box binding protein (TBP) (Santa Cruz Biotechnology Inc.) used as control of equal protein loading for cytosolic and nuclear fractions, followed by the secondary peroxidase-conjugated antibodies (Bio-Rad, Hercules, CA). To exclude nuclei-cytosol contamination, we verified that GAPDH and TBP were always undetected in nuclear and cytosolic fractions, respectively (not shown). Blot images were acquired with a ChemiDocTM Touch Imaging System device (Bio-Rad Laboratories). Densitometric analysis was performed with the ImageJ software (NIH, Bethesda, MD).

RNA extraction and quantitative real-time PCR (qRT-PCR)

Total RNA was extracted and reverse transcribed as described[2]. The qRT-PCR was performed with the iTaqTM Universal SYBR® Green Supermix (Bio-Rad). The primer sequences were designed with the qPrimerDepot software (http://primerdepot.nci.nih.gov/). The primer sequences were: *HIF-1A*: 5'-GGCTGCATCTCGAGACTTT-3': 5'-GAAGACATCGCGGGGAC; *ENO1*: 5'-GCTCCGGGACAATGATAAGA-3', 5'- TCCATCCATCTCGATCATCA-3', *GAPDH*: 5′-GAAGGTGAAGGTCGGAGT-3′, 5′-CATGGTGGAAT CATATTGGAA-3′; *VEGF*: 5'-ATCTTCAAGCCATCCTGTGTGC-3', 5'-GCTCACCGCCTCGGCTTGT-3'. The comparative CT method was used to calculate *HIF-1α*, *GLUT1*, *ENO1* and *VEGF* expression relative to the *GAPDH* product, used as a housekeeping gene, with the Bio-Rad Software Gene Expression Quantitation.

RAS and RHOA activity

The isoprenylated membrane-associated RAS or RHOA proteins and the non-

isoprenylated cytosolic forms were detected as previously described[2]. Total RAS and RHOA proteins were analyzed by WB; Briefly, the GTP-bound fraction, taken as an index of active G-proteins was measured, using a pull-down assay (with the RAF-1-GST fusion protein, agarose beads-conjugates, Millipore, Bedford, MA) and an ELISA assay (with the G-LISA™ RHOA Activation Assay Biochem Kit, Cytoskeleton Inc, Denver, CO), respectively.

Kinase inhibitors titration and kinase activity

For kinase inhibitors titration experiments we exposed CLL cells (10^6/mL) for 48 hours to PD98059, LY249002 and Y27632 at indicated increasing concentrations. ERK1-2, AKT and RHOA kinases activity was measured by spectrophotometric methods, using the CycLex RHO Kinase Assay Kit (CycLex, Nagano), the MAP Kinase/Erk Assay Kit (Millipore, Bedford, MA) and the AKT Kinase Activity Assay Kit (Abcam, Cambridge), as per manufacturer's instructions.

Cell viability assay

Cell viability was evaluated by flow cytometry using with Annexin-V/Propidium Iodide (Ann-V/PI) staining with the MEBCYTO-Apoptosis Kit (MBL Medical and Biological Laboratories, Naka-ku Nagoya). Normalized cell viability was arbitrarily defined as the ratio between the percentage of AnnV-/PI- CLL cells cultured in the presence of F-ara-A and the percentage of AnnV-/PI- CLL cells that were left untreated. CLL cells characterized by a normalized cell viability ≥0.5 were defined as *fludarabine-resistant*, otherwise, CLL cells were considered *fludarabine-sensitive*.

Table 1. Summary of genetic patient characteristics and treatment status

Unique Patient Number (UPN)	*TP53* subset	del(17)p, clone size in %	*TP53*^{mut}, allele frequency in %	IGHV mutational status	Previous Treatment
UPN01	*TP53*^{dis}	neg	mut, 84	M	y
UPN02	*TP53*^{dis}	42	mut, 83	UM	y
UPN03	*TP53*^{dis}	85	mut, 83	UM	n
UPN04	*TP53*^{dis}	80	mut, 79	UM	n
UPN05	*TP53*^{dis}	neg	mut, 75	UM	y
UPN06	*TP53*^{dis}	79	mut, 86	M	n
UPN07	*TP53*^{dis}	neg	mut, nd	UM	y
UPN08	*TP53*^{dis}	nd	mut, nd	M	nd
UPN09	*TP53*^{dis}	87	mut, 81	UM	n
UPN10	*TP53*^{dis}	neg	mut, 88	M	y
UPN11	*TP53*^{dis}	69	mut, 61	UM	y
UPN12	*TP53*^{dis}	neg	mut, 36	M	n
UPN13	*TP53*^{dis}	neg	mut, 50	M	n
UPN14	*TP53*^{dis}	24	mut, 37	UM	y
UPN15	*TP53*^{dis}	monosomy 17	mut, 50	UM	y
UPN16	*TP53*^{dis}	96	mut, 67	nd	n
UPN17	*TP53*^{dis}	neg	mut, 50	UM	y
UPN18	*TP53*^{dis}	53	mut, 31	UM	n
UPN19	*TP53*^{dis}	20	mut, 92	UM	y
UPN20	*TP53*^{dis}	88	nd	UM	n
UPN21	*TP53*^{dis}	21	mut, 25	UM	n
UPN22	*TP53*^{dis}	46	mut, 51	UM	y
UPN23	*TP53*^{dis}	70	nd	nd	y
UPN24	*TP53*^{dis}	neg	mut, 34	M	y
UPN25	*TP53*^{dis}	12	mut, 12	UM	y
UPN26	*TP53*^{dis}	neg	mut, nd	M	y
UPN27	*TP53*^{dis}	82	mut, nd	M	n
UPN28	*TP53*^{dis}	80	mut, 63	UM	y
UPN29	*TP53*^{dis}	68	mut, 75	UM	y
UPN30	*TP53*^{dis}	nd	mut, 73	nd	n
UPN31	*TP53*^{dis}	69	mut, 64	UM	n
UPN32	*TP53*^{dis}	neg	mut, nd	UM	y

UPN33	*TP53*^{dis}	43	mut, 25	M	nd
UPN34	*TP53*^{dis}	neg	mut, nd	UM	n
UPN35	*TP53*^{dis}	91	wt	M	n
UPN36	*TP53*^{dis}	59	wt	nd	n
UPN37	*TP53*^{dis}	50	wt	UM	y
UPN38	*TP53*^{dis}	50	wt	UM	y
UPN39	*TP53*^{dis}	46	wt	M	y
UPN40	*TP53*^{dis}	45	wt	M	n
UPN41	*TP53*^{wt}	neg	wt	M	y
UPN42	*TP53*^{wt}	neg	wt	M	n
UPN43	*TP53*^{wt}	neg	wt	UM	n
UPN44	*TP53*^{wt}	neg	wt	UM	n
UPN45	*TP53*^{wt}	neg	wt	M	y
UPN46	*TP53*^{wt}	neg	wt	M	y
UPN47	*TP53*^{wt}	neg	wt	M	y
UPN48	*TP53*^{wt}	neg	wt	UM	n
UPN49	*TP53*^{wt}	neg	wt	UM	n
UPN50	*TP53*^{wt}	neg	wt	M	n
UPN51	*TP53*^{wt}	neg	wt	UM	n
UPN52	*TP53*^{wt}	neg	wt	UM	y
UPN53	*TP53*^{wt}	neg	wt	UM	n
UPN54	*TP53*^{wt}	neg	wt	UM	n
UPN55	*TP53*^{wt}	neg	wt	UM	n
UPN56	*TP53*^{wt}	neg	wt	M	n
UPN57	*TP53*^{wt}	neg	wt	UM	n
UPN58	*TP53*^{wt}	neg	wt	UM	n
UPN59	*TP53*^{wt}	neg	wt	M	n
UPN60	*TP53*^{wt}	neg	wt	UM	y
UPN61	*TP53*^{wt}	neg	wt	M	n
UPN62	*TP53*^{wt}	neg	wt	M	n
UPN63	*TP53*^{wt}	neg	wt	M	y
UPN64	*TP53*^{wt}	neg	wt	UM	n
UPN65	*TP53*^{wt}	neg	wt	UM	n
UPN66	*TP53*^{wt}	neg	wt	UM	n
UPN67	*TP53*^{wt}	neg	wt	M	n
UPN68	*TP53*^{wt}	neg	wt	M	n
UPN69	*TP53*^{wt}	neg	wt	UM	n
UPN70	*TP53*^{wt}	neg	wt	nd	n

UPN71	*TP53*^{wt}	neg	wt	M	y
UPN72	*TP53*^{wt}	neg	wt	UM	n
UPN73	*TP53*^{wt}	neg	wt	UM	n
UPN74	*TP53*^{wt}	neg	wt	M	n
UPN75	*TP53*^{wt}	neg	wt	M	n
UPN76	*TP53*^{wt}	neg	wt	UM	n
UPN77	*TP53*^{wt}	neg	wt	UM	n
UPN78	*TP53*^{wt}	neg	wt	M	n
UPN79	*TP53*^{wt}	neg	wt	M	n
UPN80	*TP53*^{wt}	neg	wt	UM	n
UPN81	*TP53*^{wt}	neg	wt	M	y
UPN82	*TP53*^{wt}	neg	wt	M	n
UPN83	*TP53*^{wt}	neg	wt	M	n
UPN84	*TP53*^{wt}	neg	wt	M	n
UPN85	*TP53*^{wt}	neg	wt	nd	n
UPN86	*TP53*^{wt}	neg	wt	UM	n
UPN87	*TP53*^{wt}	neg	wt	UM	n
UPN88	*TP53*^{wt}	neg	wt	M	n
UPN89	*TP53*^{wt}	neg	wt	M	n
UPN90	*TP53*^{wt}	neg	wt	UM	n
UPN91	*TP53*^{wt}	neg	wt	nd	n
UPN92	*TP53*^{wt}	neg	wt	UM	n
UPN93	*TP53*^{wt}	neg	wt	UM	n
UPN94	*TP53*^{wt}	neg	wt	nd	n
UPN95	*TP53*^{wt}	neg	wt	UM	n
UPN96	*TP53*^{wt}	neg	wt	M	n
UPN97	*TP53*^{wt}	neg	wt	UM	n
UPN98	*TP53*^{wt}	neg	wt	UM	y
UPN99	*TP53*^{wt}	neg	wt	UM	n
UPN100	*TP53*^{wt}	neg	wt	UM	y
UPN101	*TP53*^{wt}	neg	wt	nd	n
UPN102	*TP53*^{wt}	neg	wt	M	n

Abbreviations

Del(17)p	chromosome 17p13 deletion
neg	negative, <10% del(17p)
TP53^{mut}	*TP53* gene mutation
mut	presence of *TP53* gene mutation
wt	wild type, absence of *TP53* gene mutation
nd	not determined
IGHV	Immunoglobulin heavy chian variable region genes

M	IGHV mutated
UM	IGHV unmutated

Supplemental Figures

Supplemental Figure 1

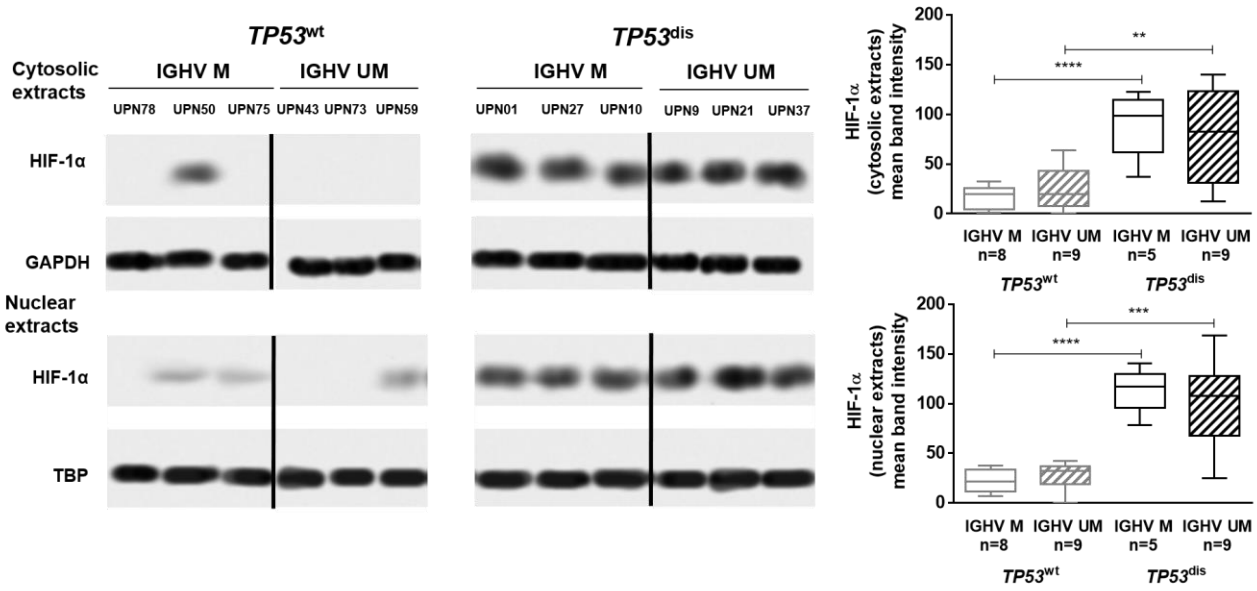

Figure S1. The association between HIF-1α expression and the *TP53* status is not influenced by the IGHV mutational status. The expression of HIF-1α was measured in *TP53*^{wt} and *TP53*^{dis} CLL cells, accounting for the IGHV mutational status. *TP53*^{wt} CLL included 8 IGHV M and 9 IGHV UM samples, and *TP53*^{dis} CLL included 5 IGHV M and 8 IGHV UM samples. A representative blot is shown, together with Unique Patients Number (UPN) and cumulative band intensity data obtained from the analysis of the four subsets (i.e. *TP53*^{wt}/IGHV M, *TP53*^{wt}/IGHV UM, *TP53*^{dis}/IGHV M and *TP53*^{dis}/IGHV UM CLL patients). Box plots represent median values and 25%-75% percentiles, whiskers represent minimum and maximum values of band intensity for each group. Vertical lines have been inserted to indicate repositioned gel lanes. **** p<0.0001, *** p<0.001, ** p<0.01.

Supplemental Figure 2

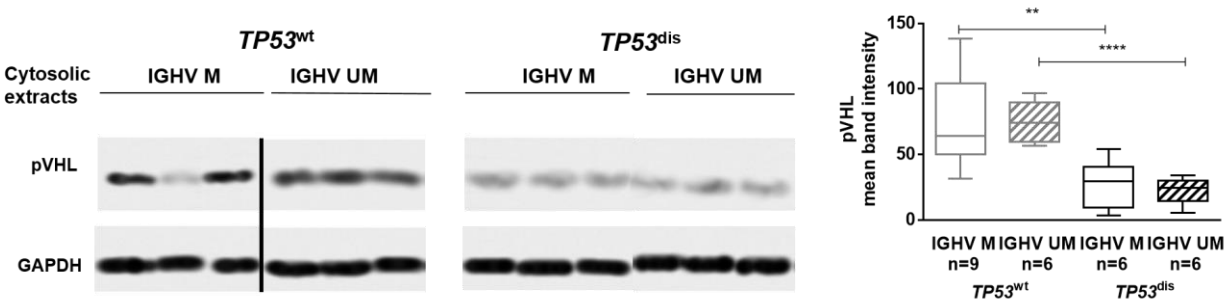

Figure S2. The expression of pVHL is not influenced by IGHV mutational status.

The expression of pVHL was measured in *TP53*^{wt} and *TP53*^{dis} CLL cells, accounting for the IGHV mutational status. *TP53*^{wt} CLL included 9 IGHV M and 6 IGHV UM samples, and *TP53*^{dis} CLL included 6 IGHV M and 6 IGHV UM samples. A representative blot is shown, together with UPN and cumulative band intensity data obtained from the analysis of the four subsets. Box plots represent median value and 25%-75% percentiles, whiskers represent minimum and maximum values of band intensity for each group. Vertical lines have been inserted to indicate repositioned gel lanes. **** $p<0.0001$, ** $p<0.01$.

Supplemental Figure 3

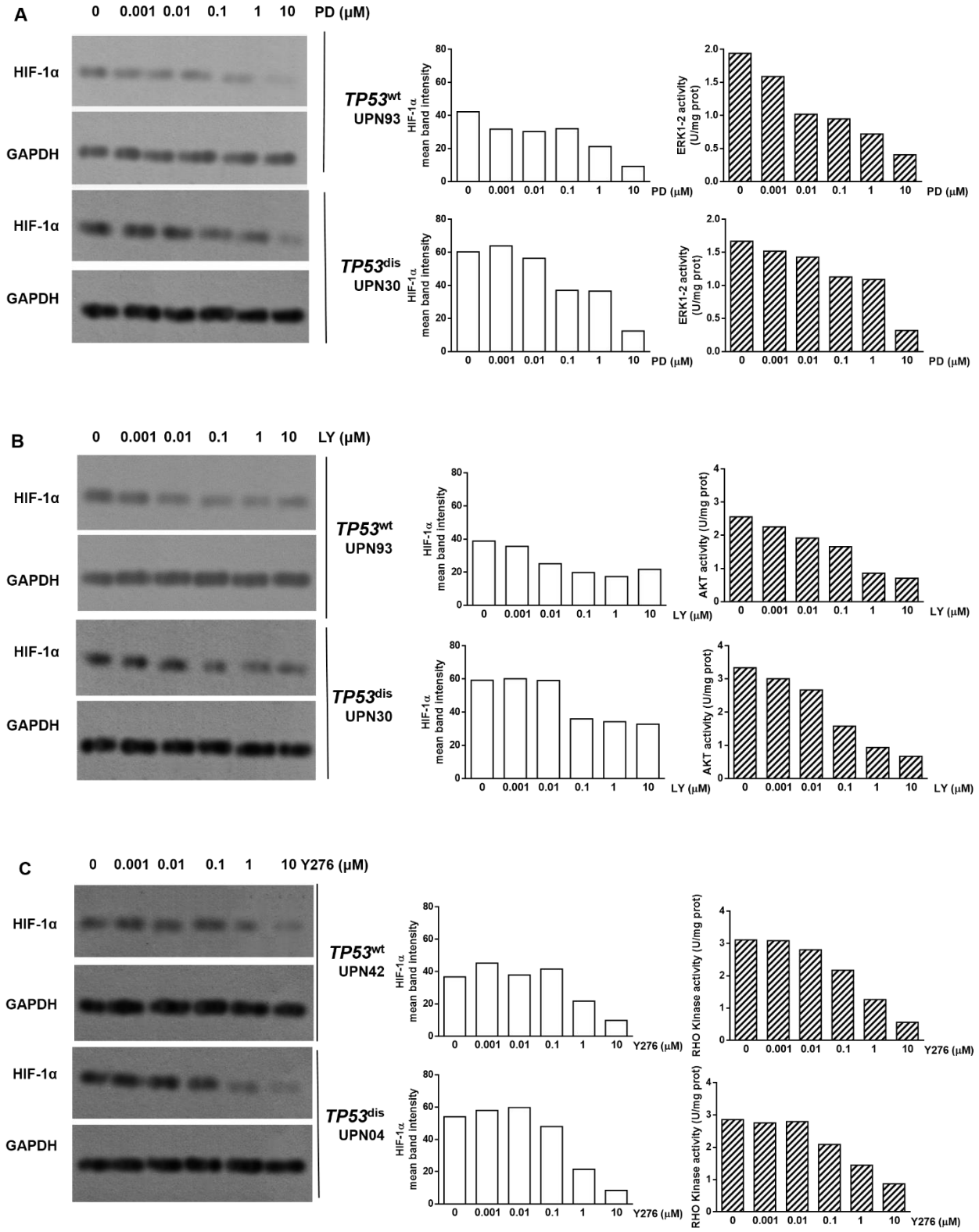

Figure S3. Increasing concentrations of ERK1-2, PI3K or RHOA kinase inhibitors determine a progressive reduction of HIF-1α levels. Primary CLL cells were cultured for 48 hours in the presence of increasing concentration of PD98059 (PD, 0.01 μM, 0.1 μM, 1 μM or 10 μM) **(A)**, LY294002 (LY, 0.01 μM, 0.1 μM, 1 μM or 10 μM) **(B)** or Y27632 (Y276 0.01 μM, 0.1 μM, 1 μM or 10 μM) **(C)**. WB analyses of HIF-1α protein expression for 1 *TP53*^{wt} and 1 *TP53*^{dis} representative CLL patient, together with UPN and the corresponding cumulative band intensity data, are shown. ERK1-2, AKT and RHOA kinase activities were evaluated by an immunomediated assay and are shown by bar graphs on the right.

Supplemental Figure 4

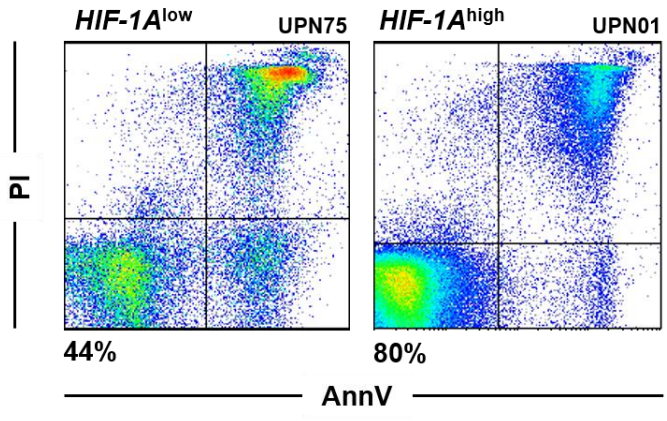

Figure S4. Viability of *HIF-1A*^{high} and *HIF-1A*^{low} CLL cells. Representative flow cytometry analysis (relative UPN indicated) of AnnV/PI expression on *HIF-1A*^{high} and *HIF-1A*^{low} CLL cells after 48-hour culture in medium. CLL cells isolated from *HIF-1A*^{high} samples had a significantly higher viability than CLL cells isolated *HIF-1A*^{low} samples.

Supplemental Figure 5

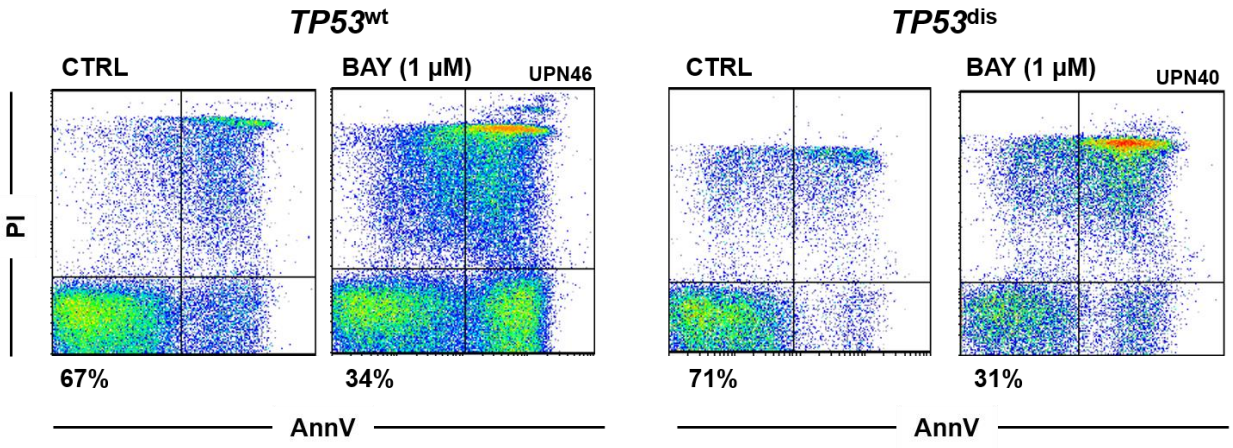

Figure S5. Viability of *TP53*^{wt} and *TP53*^{dis} CLL cells exposed to BAY87-2243. Representative flow cytometry analysis (relative UPN indicated) of AnnV/PI expression on *TP53*^{wt} and *TP53*^{dis} CLL cells exposed to 1 µM BAY87-2243 (BAY) or left untreated for 48 hours. BAY87-2243 determined a direct cytotoxic effect toward leukemic cells isolated from both patient subsets.

Supplemental Figure 6

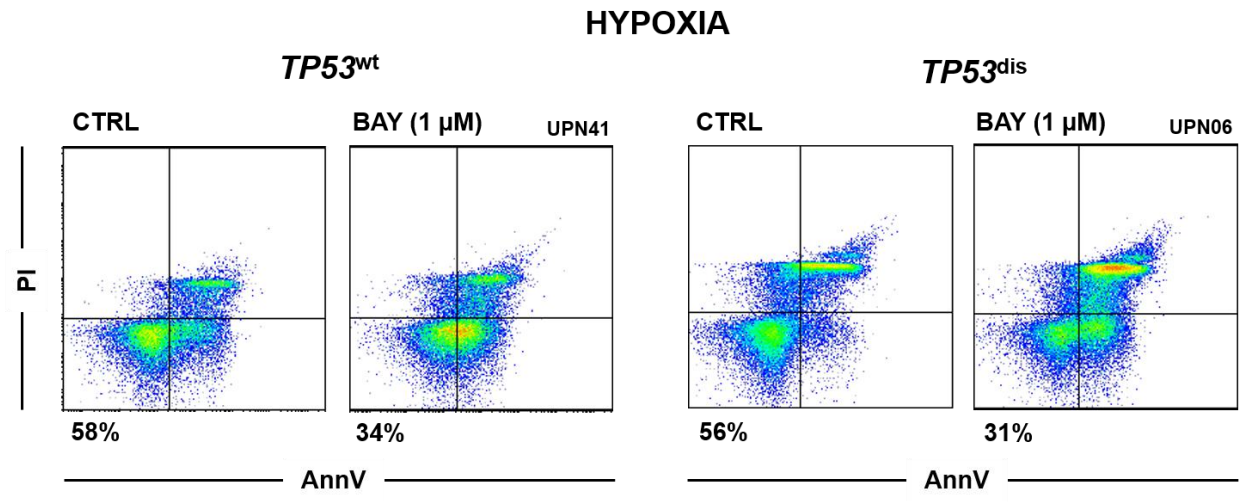

Figure S6. Viability of *TP53*^{wt} and *TP53*^{dis} CLL cells exposed to BAY87-2243 under hypoxia. Representative flow cytometry analysis (relative UPN indicated) of AnnV/PI expression on *TP53*^{wt} and *TP53*^{dis} CLL cells exposed to 1 µM BAY87-2243 (BAY) or left untreated for 48 hours, under hypoxic conditions. BAY87-2243 exerted a cytotoxic effect also when *TP53*^{dis} and *TP53*^{wt} CLL cells were cultured in conditions of hypoxia.

Supplemental Figure 7

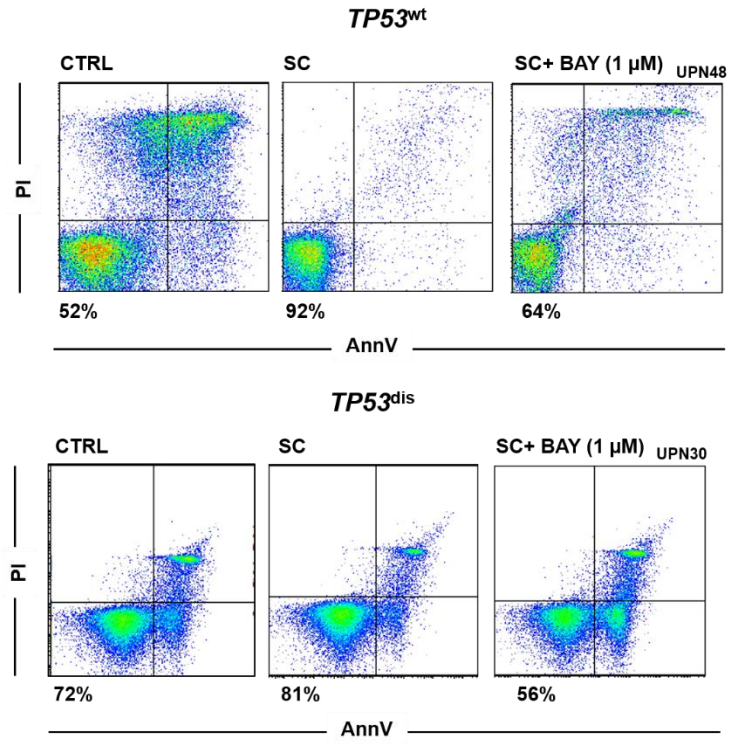

Figure S7. Viability of *TP53*^{wt} and *TP53*^{dis} CLL cells exposed to BAY87-2243 in presence of SC. Representative flow cytometry analysis (relative UPN indicated) of AnnV/PI expression on *TP53*^{wt} and *TP53*^{dis} CLL cells exposed to 1 µM BAY87-2243 (BAY) or left untreated for 48 hours, in the presence or in the absence of the murine SC line M2-10B4. BAY87-2243 exerted a cytotoxic effect also when *TP53*^{dis} and *TP53*^{wt} CLL cells were co-cultured with SC.

Supplemental Figure 8

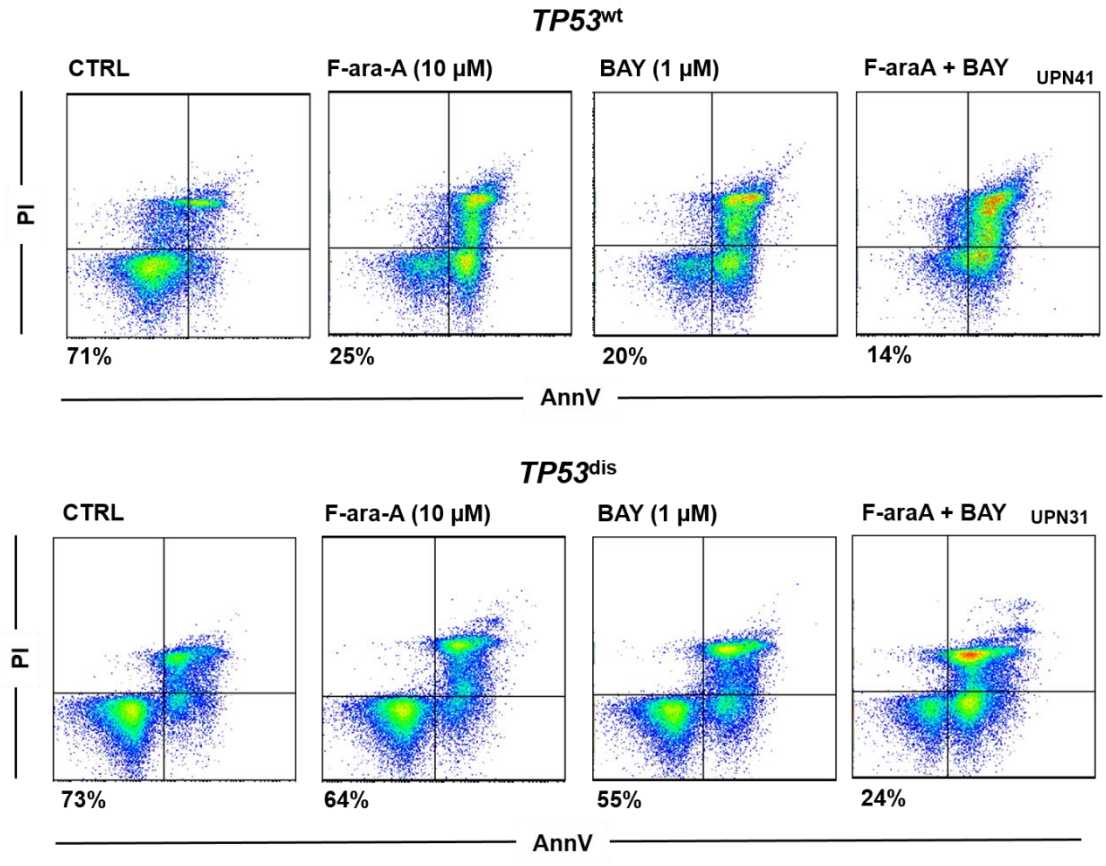

Figure S8. Viability of *TP53*^{wt} and *TP53*^{dis} CLL cells exposed to BAY87-2243 + fludarabine. Representative flow cytometry analysis (relative UPN indicated) of AnnV/PI expression on *TP53*^{dis} and *TP53*^{wt} CLL cells exposed for 48 hours to 1 μM BAY87-2243 (BAY) and/or 10 μM F-ara-A. The combination BAY87-2243 + F-ara-A determined a significant decrease in the viability of *TP53*^{wt} and *TP53*^{dis} CLL cells, compared to each compound used as single agent and to untreated controls.

Supplemental Figure 9

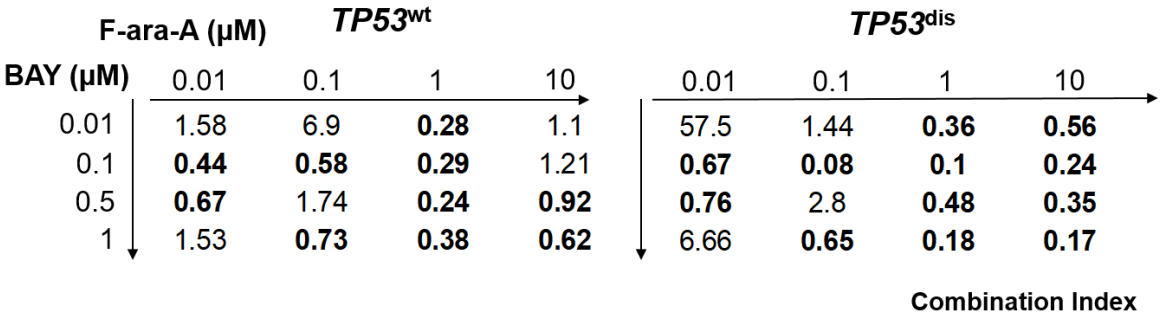

Figure S9. CI of BAY87-2243 + fludarabine combinations. Figure showing combination indexes (CI) relative to 48-hour treatment with BAY87-2243 (BAY) and F-ara-A, used at different concentrations in *TP53*^{wt} and *TP53*^{dis} CLL cells. CI<1, highlighted in bold, indicate synergistic combinations.

Supplemental Figure 10

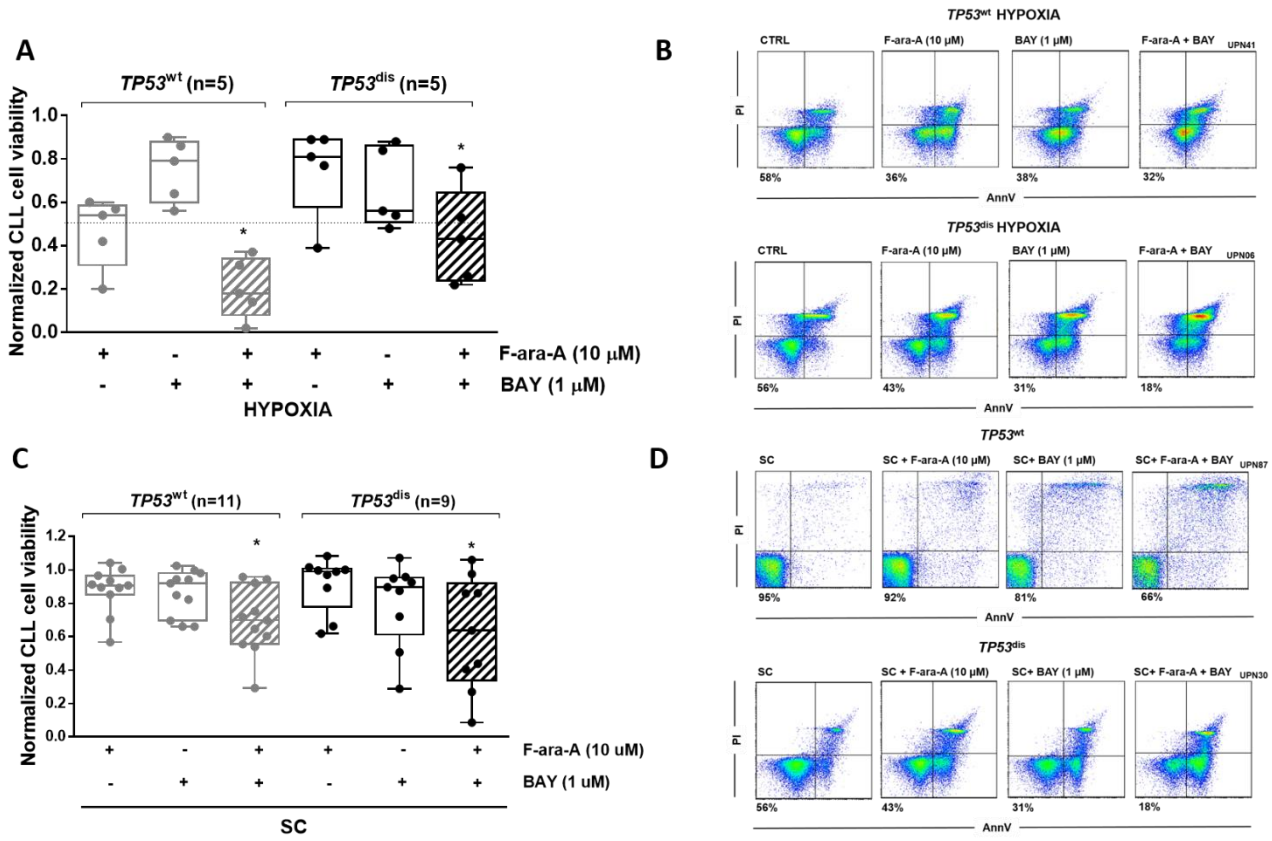

Figure S10. BAY87-2243 + fludarabine combination exerts a significant cytotoxic effect on *TP53*^{dis} and *TP53*^{wt} CLL cultured under hypoxia or in the presence of SC. Normalized cell viability of *TP53*^{dis} and *TP53*^{wt} CLL cells exposed for 48 hours to 1 μM BAY87-2243 (BAY) and/or 10 μM F-ara-A, under normoxia and hypoxia, or in co-culture with SC. The combination BAY87-2243 + F-ara-A (striped pattern) determined a significant decrease in the viability of *TP53*^{wt} and *TP53*^{dis} CLL cells, compared to each compound used as single agent, in condition of hypoxia **(A, B)** or in the presence of SC **(C, D).** In panels A and C, box plots represent median values and 25%-75% percentiles, whiskers represent minimum and maximum values for each group, together with all the points. In panels B and D, representative flow cytometry analysis (relative UPN indicated) of

AnnV/PI expression on *TP53*^{dis} and *TP53*^{wt} CLL cells exposed for 48 hours to 1 μM BAY87-2243 and/or 10 μM F-ara-A in the presence of SC.

Supplemental Figure 11

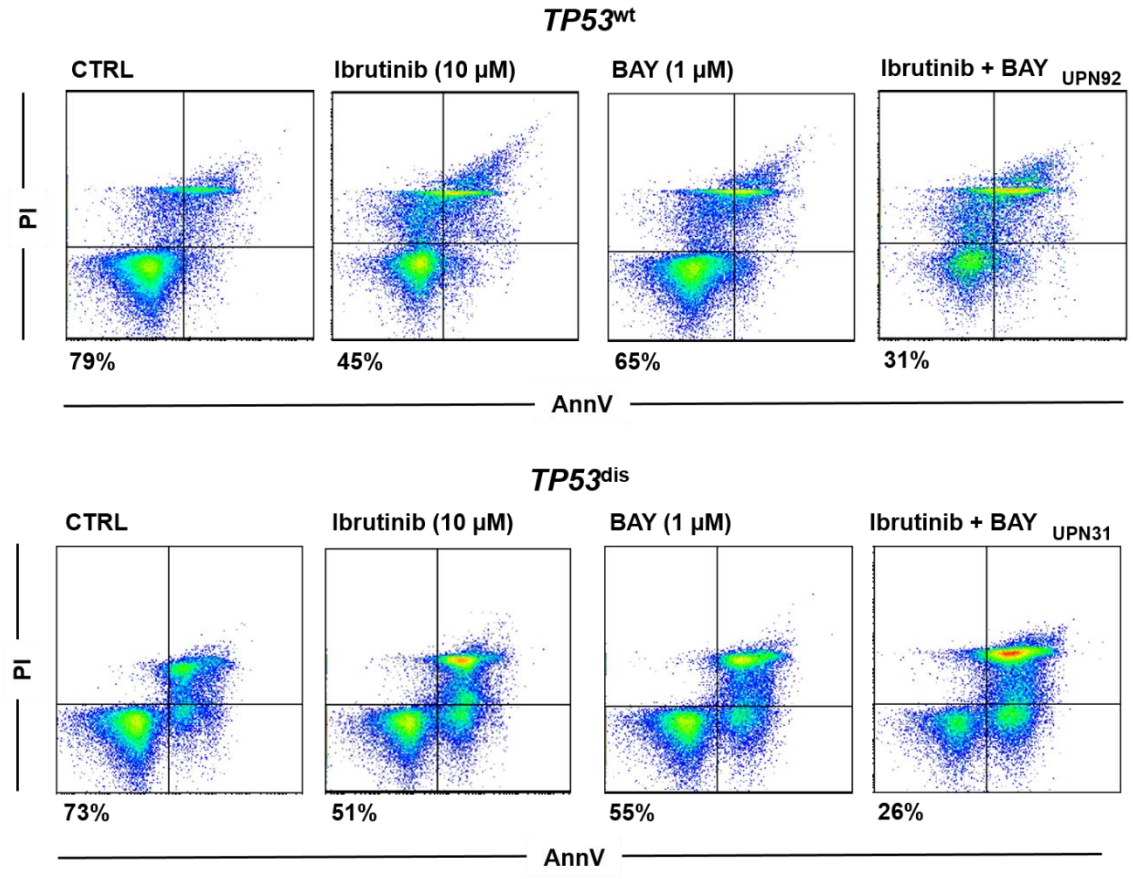

Figure S11. Viability of *TP53*^{wt} and *TP53*^{dis} CLL cells exposed to BAY87-2243 + ibrutinib. Representative flow cytometry analysis (relative UPN indicated) of AnnV/PI expression on *TP53*^{dis} and *TP53*^{wt} CLL cells exposed for 48 hours to 1 μM BAY87-2243 (BAY) and/or 10 μM ibrutinib. The combination BAY87-3342 + ibrutinib determined a significant decrease in the viability of *TP53*^{wt} and *TP53*^{dis} CLL cells, compared to each compound used as single agent and to untreated controls.

Supplemental Figure 12

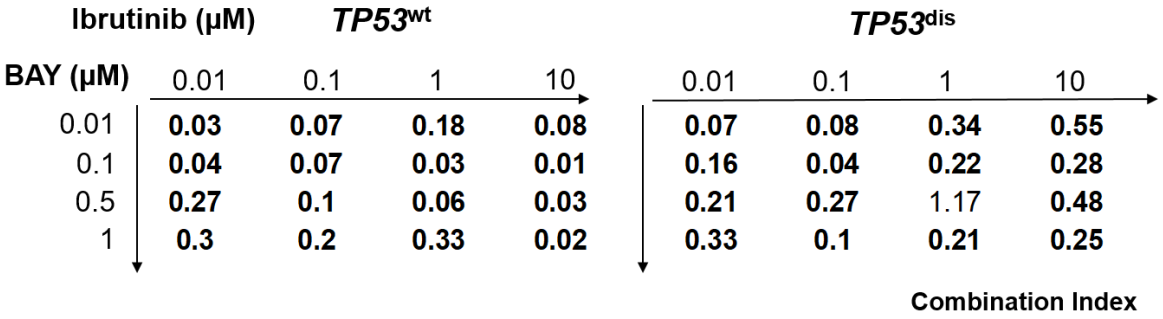

Figure S12. CI of BAY87-2243 + ibrutinib combinations. Figure showing combination indexes (CI) relative to the 48-hour treatment with BAY87-2243 (BAY) and ibrutinib, used at different concentrations in *TP53*^{wt} and *TP53*^{dis} CLL cells. CI<1, highlighted in bold, indicate synergistic combinations.

Supplemental references

1. Ricca I, Rocci A, Drandi D, et al. Telomere length identifies two different prognostic subgroups among VH-unmutated B-cell chronic lymphocytic leukemia patients. Leukemia 2007;21(4):697–705.

2. Rigoni M, Riganti C, Vitale C, et al. Simvastatin and downstream inhibitors circumvent constitutive and stromal cell-induced resistance to doxorubicin in IGHV unmutated CLL cells. Oncotarget 2015;6(30):29833–29846.